Karlsruher Institut für Technologie

Report on Project 5: Particle Simulation

Lars Biebinger and Hermann Gegel

28.05. - 26.07.2019

Team 2: Numerical Analysis of Partial Differential Equations
Institute of Applied and Numerical Mathematics
Karlsruhe Institute of Technology

Supervision: Robin Trunk & Fabian Klemens

Contents

Abbreviations I

Symbols II

1 Introduction 1

2 Theoretical Background 2
- 2.1 Mathematical Modelling . . . 2
- 2.2 Numerical Methods . . . 3
- 2.3 Particles in HLBM . . . 7

3 Collision of Two Spheres 8
- 3.1 Study of the initial setup . . . 8
  - 3.1.1 Variation of Epsilon . . . 9
  - 3.1.2 Variation of the Particle Density . . . 12
  - 3.1.3 Variation of the Initial Velocity . . . 14
- 3.2 Collision with both Spheres in Motion . . . 16
- 3.3 Oblique Impact . . . 18

4 Conclusion 20

5 Appendix 21

Abbreviations

Abbreviation	Term
BGK	Bhatnagar, Gross and Krook
BE	Boltzmann equation
HLBM	Homogenised lattice Boltzmann method
LBE	Lattice Boltzmann equation
LBM	Lattice Boltzmann method
MEA	Momentum exchange algorithm
NSE	Navier-Stokes equation
PDE	Partial differential equation
SPH	Smooth-Particle-Hydrodynamics
STP	Standard conditions for temperature and pressure

Symbols

Symbol	Term
ω_i	Angular speed of i
ϵ	Arbitrary parameter (≥ 0)
$\mathbf{X}_i$	Center of mass of i
u_{lb}	Characteristic lattice velocity
$\Omega(f)$	Collision operator
$\overline{\mathbf{u}}_i$	Convex combination of fluid velocity and rigid-body velocity
ρ	Density
f_i	Discrete distribution function
c_i	Discrete mesoscopic velocity
f	Distribution function
f^{eq}	Equilibrium distribution function
F_i	Force i
ν	Kinematic viscosity
d	Level-set function connected to moving porosity
$\mathbf{u}_i$	Macroscopic velocity of i
j	Mass flux density
m_i	Mass of i
$\mathbf{J}_i$	Moment of inertia acting on i
$\mathbf{g}_i$	Momentum exchange
$\mathbf{x}$	Position in macroscopic space
d_k	Porosity
p	Pressure
R_i	Radius of i
τ	Relaxation time
N	Resolution parameter
Re	Reynolds number
p_h	Set of nodes inside the particle boundary
ϵ_h	Smoothing parameter
h	Spacing
c_s	Speed of sound
s	Supporting function for d
t	Time
$\mathbf{T}_i$	Torque i
ξ	Velocity space
w_i	weight of c_i

1 Introduction

With the growth of the quaternary sector of economy due to consumer and market demand society is currently facing a rapid increase in computing power. Hence several new approaches to solve computationally intensive problems are emerging, which is especially convenient for scientific research. The primary goals are to replace expensive and time-consuming experiments with numerical simulations as well as opening the door to knowledge, that is otherwise unattainable without high computation power and cunning algorithms. For fluid mechanic problems this numerical analysis is known as Computational Fluid Dynamics (CFD). It is a collocation of different models to predict the behavior of pure fluids or multi-phase flows. Usually the reviewed fluid is seen as a continuum and calculated via Navier-Stokes equations (NSE). However, this approximation on a macroscopic scale is connected to several assumptions deviating from reality. At the same time it is impossible to simulate the movement of every single molecule. Therefore it is desirable to implement a mesoscopic model to assure accuracy while maintaining comparatively low computational intensity. This can be achieved with lattice Boltzmann methods (LBM) which describe fluids via statistical physics. For this purpose the material balance envelope is defined on a homogenous grid with particle populations on the nodes. Fluid movements are calculated with an explicit scheme of collision and streaming steps. The major advantages of LBM are its computational efficiency and parallel scalability. This makes it especially suitable for the simulation of particle-fluid systems, which are receiving a lot of attention due to the relevance of suspensions in technical applications. In contrast to other Smooth-Particle-Hydrodynamics (SPH) methods, where usually an Eulerian grid is deployed for the fluid phase and the particles are defined on a Lagrangian grid, both fluid and solid phase are defined on a single grid. Based on the chosen boundary conditions this can save a lot of computing time, as no extensive interpolations are needed (cf. "Immersed Boundary method" [2, 7]). Recently a new approach referred to as the homogenized lattice Boltzmann method (HLBM) was published by Krause et al. [3]. It extends the model for flow through static porous media by Spaid and Phelan [8] with a momentum exchange algorithm (MEA) proposed by Ladd [5, 6] in order to simulate moving porous media. The porosity is modelled by implementing a smooth transition zone between solid and fluid phase. The smoothing parameter helps to avoid pressure fluctuations and ensures stable momentum transfer between fluid and solid phase calculated by Ladd's MEA. This approach has shown to provide physically plausible results although no additional collision model is incorporated [3, 9].
In this study we further investigate the physical plausibility of the HLBM by simulating a collision between two spheres in a three-dimensional space. The results are depicted by plotting velocity and force over time and visualizing the collision at discrete time steps via ParaView.

2 Theoretical Background

2.1 Mathematical Modelling

In order to investigate the behavior of multi-phase flows it is necessary to solve mathematical equations which model the physical properties of the observed system. The fluid phase is specified by the incompressible Navier-Stokes equation (NSE) given by

$$\frac{\partial \mathbf{u}_f}{\partial t} + (\mathbf{u}_f \cdot \nabla)\mathbf{u}_f - \nu \Delta \mathbf{u}_f + \frac{1}{\rho_f}\nabla p = \mathbf{F}_f \tag{1}$$

$$\nabla \cdot \mathbf{u}_f = 0. \tag{2}$$

Eq. (1) depicts the change of net momentum for a fluid element, while considering irreversible momentum transfer due to internal friction and external forces acting on the fluid. For an incompressible fluid the mass conservation is given by the continuity equation (see Eq. (2)). In order to solve these partial differential equations it is necessary to define initial and boundary conditions specifying the system. The motion of particles is described by rigid-body dynamics derived from Newton's second law of motion. The relevant equations are given by

$$m_p \frac{\partial \mathbf{u}_p(t)}{\partial t} = \mathbf{F}_p(t) \tag{3}$$

$$\mathbf{J}_p \frac{\partial \boldsymbol{\omega}_p(t)}{\partial t} = \mathbf{T}_p(t). \tag{4}$$

Here $\mathbf{F}_p$ and $\mathbf{T}_p$ are the entities of forces and torque acting on the particle. In this study, no additional collision model is implemented and gravitational forces are neglected due to the miniscule time frame. Therefore $\mathbf{F}_p$ corresponds to the hydrodynamic force $\mathbf{F}_h$ and the torque $\mathbf{T}_p$ derives from $\mathbf{F}_h$ and its point of application on the particle. The connection between the basic equations (1)-(4) and the numerical implementation is specified in the following section.

2.2 Numerical Methods

The HLBM is an extension of a classic lattice Boltzmann model, which enables the simulation of moving porous media in a fluid. The adaptions applied to the Boltzmann equation (BE) are presented in this section.
The fluid phase is described by a distribution function of fluid particles $f(\mathbf{x}, \boldsymbol{\xi}, t)$ originated from the kinetic theory. The total derivative of $f(\mathbf{x}, \boldsymbol{\xi}, t)$ with respect to time recovers the classic Boltzmann equation:

$$\underbrace{\left(\frac{\partial}{\partial t} + \boldsymbol{\xi} \cdot \nabla\right)}_{A} + \underbrace{\frac{\mathbf{F}}{\rho_f} \cdot \nabla_\xi}_{B} \Big) f = \underbrace{\Omega(f)}_{C} \tag{5}$$

A: convective forces originated from the microscopic particle velocity
B: external forces affecting the microscopic particle velocity
C: collision operator

In order to solve the equation numerically it is necessary to implement a discretized Boltzmann equation. For the discretization of the spatial domain there are several common sets of discrete mesosopic velocities c_i denoted as $DdQq$, where d marks the dimension and q the number of velocities. A schema for the $D3Q19$ discretization which was used in this study is given in Fig. 1.

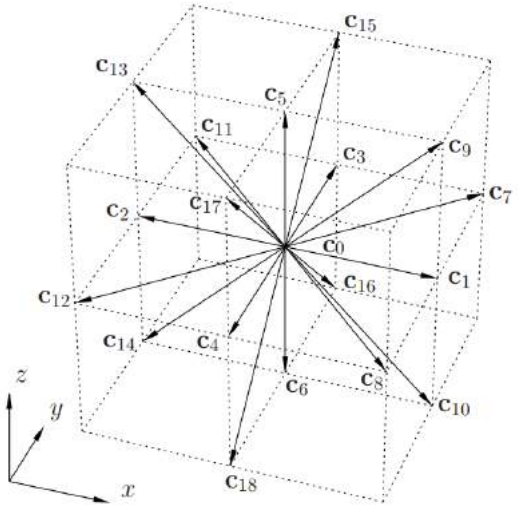

Figure 1: Discretization of the spatial domain and the velocity space for a $D3Q19$ lattice [2].

By using such a homogeneous grid with spacing $h \, \epsilon \, \mathbb{R}_{>0}$ for the discretization one recovers the lattice Boltzmann equation (LBE):

$$f_i(\mathbf{x} + \mathbf{c}_i h^2, t + h^2) - f_i(\mathbf{x}, t) = -\frac{1}{\tau}\Big(f_i(\mathbf{x}, t) - f_i^{eq}(\rho, \overline{\mathbf{u}})\Big) \tag{6}$$

$$\Omega_{BGK}(f) = -\frac{1}{\tau}\Big(f_i(\mathbf{x},t) - f_i^{eq}(\rho,\overline{\mathbf{u}})\Big). \tag{7}$$

This equation is build upon the theory that the particle density distributions converge towards a local equilibrium function f_i^{eq} through collisions. In the LBE this process is often depicted by the BGK collision operator Ω_{BGK} first proposed by Bhatnagar, Gross and Krook [1]. It is an approximation of the complicated original collision operator proposed by Boltzmann. The relaxation time τ determines the transport coefficients and thus the speed of equilibration which makes it crucial for the stability of the simulation. It is connected to the macroscopic value of the fluid's kinematic viscosity via $\nu = c_s^2(\tau - \frac{\Delta t}{2})$ [4]. In order to implement the LBE it is usually divided into two steps:

1. collision step: relaxes the distribution functions f_i at each lattice node towards its corresponding local equilibrium function f_i^{eq}.

$$\tilde{f}_i(\mathbf{x},t) = f_i(\mathbf{x},t) - \frac{1}{\tau}\Big(f_i(\mathbf{x},t) - f_i^{eq}(\rho,\overline{\mathbf{u}})(\mathbf{x},t)\Big) \tag{8}$$

2. streaming step: propagates each distribution function f_i to the next lattice node in the direction of its assigned lattice vector c_i.

$$f_i(\mathbf{x} + \mathbf{c}_i h^2, t + h^2) = \tilde{f}_i(\mathbf{x},t) \tag{9}$$

Considering this calculation routine and the definition of $\Omega_{BGK}(f)$ it is obvious that the BGK collision operator only depends on the local values of f_i. This makes the observed system divisible into separately calculable sections and is the basis for efficient parallel computing. The equilibrium function f_i^{eq} given throughout the equations (6)-(8) is a discrete Maxwell-Boltzmann distribution and describes the thermodynamic equilibrium of the observed system. It is given by

$$f_i^{eq}(\rho,\overline{\mathbf{u}}) = w_i\rho\left(1 + \frac{\overline{\mathbf{u}}\cdot\mathbf{c}_i}{c_s^2} + \frac{(\overline{\mathbf{u}}\cdot\mathbf{c}_i)^2}{2c_s^4} - \frac{\overline{\mathbf{u}}\cdot\overline{\mathbf{u}}}{2c_s^2}\right). \tag{10}$$

Every velocity c_i is assigned a weight w_i. These weights' values depend on the chosen discretization and determine the contribution of each velocity c_i to its corresponding equilibrium distribution function.

$$w_i = \begin{cases} \frac{1}{3}, & i = 0 \\ \frac{1}{18}, & i = 1\ldots5 \\ \frac{1}{36}, & i = 6\ldots18 \end{cases}$$

$$c_i = \begin{cases} (0,0,0), & i = 0 \\ \left(\pm\frac{1}{h},0,0\right), \left(0,\pm\frac{1}{h},0\right), \left(0,0,\pm\frac{1}{h}\right), & i = 1\ldots5 \\ \left(\pm\frac{1}{h},\pm\frac{1}{h},0\right), \left(\pm\frac{1}{h},0,\pm\frac{1}{h}\right), \left(0,\pm\frac{1}{h},\pm\frac{1}{h}\right), & i = 6\ldots18 \end{cases}$$

In order to consider the porosity of the moving media we introduce the macroscopic velocity $\overline{\mathbf{u}}$ as a convex combination of the fluid velocity $\mathbf{u}_f$ and the rigid-body velocity $\mathbf{u}_b$ given in Eq. (11). The correlation between the macroscopic rigid-body velocity $\mathbf{u}_b$ and the microscopic velocity of the particles $\mathbf{u}_k^p$ is shown in Eq. (12) and (13). Hereby the translational and angular velocities of the particles are considered. The connection between meso- and macroscopic scale for the fluid phase is given through the moments of the particle distribution function f_i as shown in Eq. (14) and (15).

$$\bar{\mathbf{u}} = \mathbf{u}_f(\mathbf{x},t) + d(\mathbf{x},t)(\mathbf{u}_b(\mathbf{x},t) - \mathbf{u}_f(\mathbf{x},t)) \tag{11}$$

$$\mathbf{u}_b(\mathbf{x},t) = \frac{\sum_k d_k(\mathbf{x},t)\mathbf{u}_k^p(\mathbf{x},t)}{\sum_k d_k(\mathbf{x},t)} \tag{12}$$

$$\mathbf{u}_k^p(\mathbf{x},t) = \overline{\mathbf{u}}_k^p + \boldsymbol{\omega}_k(t) \times (\mathbf{x} - \mathbf{X}_k(t)) \tag{13}$$

$$\mathbf{u}_f(\mathbf{x},t) = \frac{1}{\rho(\mathbf{x},t)} \sum_{i=0}^{q} f_i(\mathbf{x},t)\mathbf{c}_i \tag{14}$$

$$\rho(\mathbf{x},t) = \sum_{i=0}^{q} f_i(\mathbf{x},t) \tag{15}$$

This approach, based on a study proposed by Krause et al. [3], allows us to differentiate between nodes representing fluid, solid and transitional domains. For this purpose a level-set function $d(\mathbf{x},\mathbf{t}) \in [0,1]$ is established. For $d(\mathbf{x},t) = 0$ the velocity $\bar{\mathbf{u}}$ corresponds to a classic BGK-LBM fluid calculation and for $d(\mathbf{x},t) = 1$ we obtain a pure solid medium respectively. Depending on the values of the rigid-body velocity $\mathbf{u}_b$ and $d(\mathbf{x},t)$ we distinguish between two cases:

1. For $\mathbf{u}_b = 0$ the node represents a static porous medium (for details see [8]).
2. In HLBM, the $\mathbf{u}_b$ is arbitrary and can be seen as flow through moving porous and solid media.

On each lattice node the parameter $d(\mathbf{x}, t)$ is computed by

$$d(\mathbf{x}, t) = 1 - \prod_{k=0}^{N} d_k(\mathbf{x}, t) \tag{16}$$

with porosity d_k. The porosity needs to be modeled according to the shape of the particle. For a spherical particle with center of mass $\mathbf{X}_k(t)$, radius R_k, $R_k^+ = R_k + \frac{\epsilon_h}{2}$ and $R_k^- = R_k - \frac{\epsilon_h}{2}$

$$d_k(\mathbf{x}, t) = \begin{cases} 1, & \|\mathbf{x} - \mathbf{X}_k(t)\|_2 \leq R_k^- \\ \cos^2\left(\frac{\pi}{2\epsilon_h}(\|\mathbf{x} - \mathbf{X}_k(t))\|_2 - R_k^+)\right), & R_k^- < \|\mathbf{x} - \mathbf{X}_k(t)\|_2 \leq R_k^+ \\ 0, & \|\mathbf{x} - \mathbf{X}_k(t))\|_2 > R_k^+ \end{cases} \tag{17}$$

with a smoothing parameter $\epsilon_h = \epsilon h$, where $\epsilon \geq 0$ is an arbitrary parameter. It scales the transition zone for the parameter d proportionately to the spacing parameter h. This helps to avoid pressure fluctuations and thus ensures numerical stability. A sharp boundary is obtained when h approaches zero. A visualization is depicted in Fig. 2.

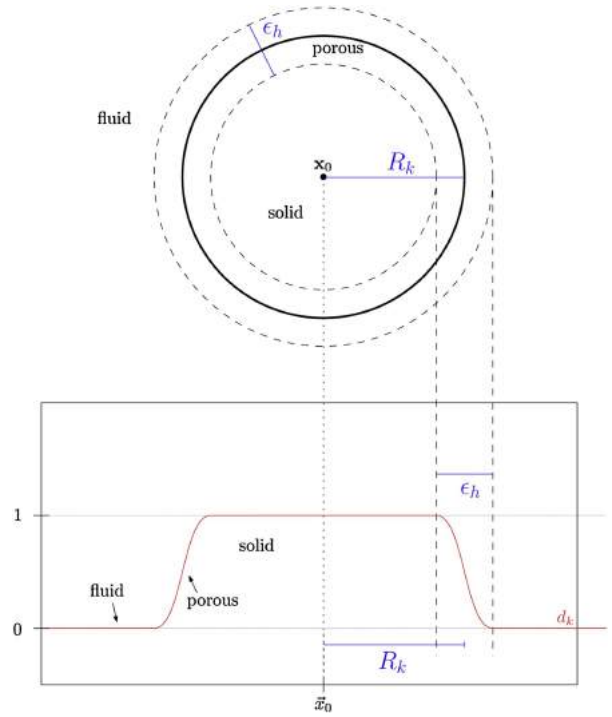

Figure 2: Visualization of the smooth transition of parameter d_k, taken from [3]. It shows the values of the porosity d_k as a function of the distance to the sphere center x_0 for a sphere with radius R_k. Outside the particle: $d_k = 0$, inside the particle: $d_k = 1$, transition zone for $\epsilon_h \geq 0$: $0 \leq d_k \leq 1$.

2.3 Particles in HLBM

The fluid-particle interaction is included in the lattice Boltzmann equation through an alteration of the velocity (see Eq. 11). This interaction leads to a momentum loss, which can be viewed as an external balancing force acting on the particle [9]. To ensure the conservation of total momentum in the system the momentum exchange algorithm (MEA) proposed by Ladd (see [5, 6]) and extended by Krause et al. [3] is utilized. The momentum exchange of a node $\mathbf{x}$ with its neighboring node $\mathbf{x} + \mathbf{c}_i h^2$ are calculated by

$$\mathbf{g}_i(\mathbf{x}, t) = \mathbf{c}_i f_i(\mathbf{x}, t) + \mathbf{c}_i^* f_i^*(\mathbf{x} + \mathbf{c}_i h^2, t) \tag{18}$$

with $c_i^* = -c_i$ and f_i^* depicting the distribution function f_i in the reverse direction. The momentum exchange happens in the whole transition zone, therefore the hydrodynamic force $\mathbf{F}_h$ and torque $\mathbf{T}_h$ acting on the particle is calculated by

$$\mathbf{F}_h(\mathbf{x}, t) = \sum_{\mathbf{x} \epsilon p_h} s(\mathbf{x}, t) \sum_i \mathbf{g}_i(\mathbf{x}, t) \tag{19}$$

and

$$\mathbf{T}_h(\mathbf{x}, t) = \sum_{\mathbf{x} \epsilon p_h} s(\mathbf{x}, t)(\mathbf{x} - \mathbf{X}_p(t)) \sum_i \mathbf{g}_i(\mathbf{x}, t) \tag{20}$$

with p_h as the set of nodes inside the particle boundary and the supporting function $s(\mathbf{x}, t)$ for $d(\mathbf{x}, t)$

$$s(\mathbf{x}, t) = \begin{cases} 1, \ d(\mathbf{x}, t) > 0, \\ 0, \ d(\mathbf{x}, t) = 0. \end{cases} \tag{21}$$

To update the position and velocity of the particles, the Verlet algorithm given by

$$\mathbf{X}_p(t + h^2) = \mathbf{X}_p(t) + \mathbf{u}_p(t) h^2 + \frac{1}{m_p} \mathbf{F}_p(t) h^4 \tag{22}$$

$$\mathbf{u}_p(t + h^2) = \mathbf{u}_p(t) + \frac{\mathbf{F}_p(t) + \mathbf{F}_p(t + h^2)}{2 m_p} h^2 \tag{23}$$

with $\mathbf{F}_p$ as the total force acting on the particle is used. As it was pointed out in section 2.1, only the hydrodynamic force acting on the particle is relevant in this study.

3 Collision of Two Spheres

The examined case in the course of this project was the collision of two spheres in a 3D domain of a viscous fluid. The initial set up is depicted in Fig. 3. The domain has a dimension of $0.03m \times 0.01m \times 0.01m$. The fluid has a kinematic viscosity $\nu = 1 \cdot 10^{-5} \frac{N}{m^2}$. The gravitational acceleration as well as buoyancy is neglected, because the collision happens in a small time frame ($t_{coll} \approx 0.02s$). In addition a perfectly inelastic collision was assumed.

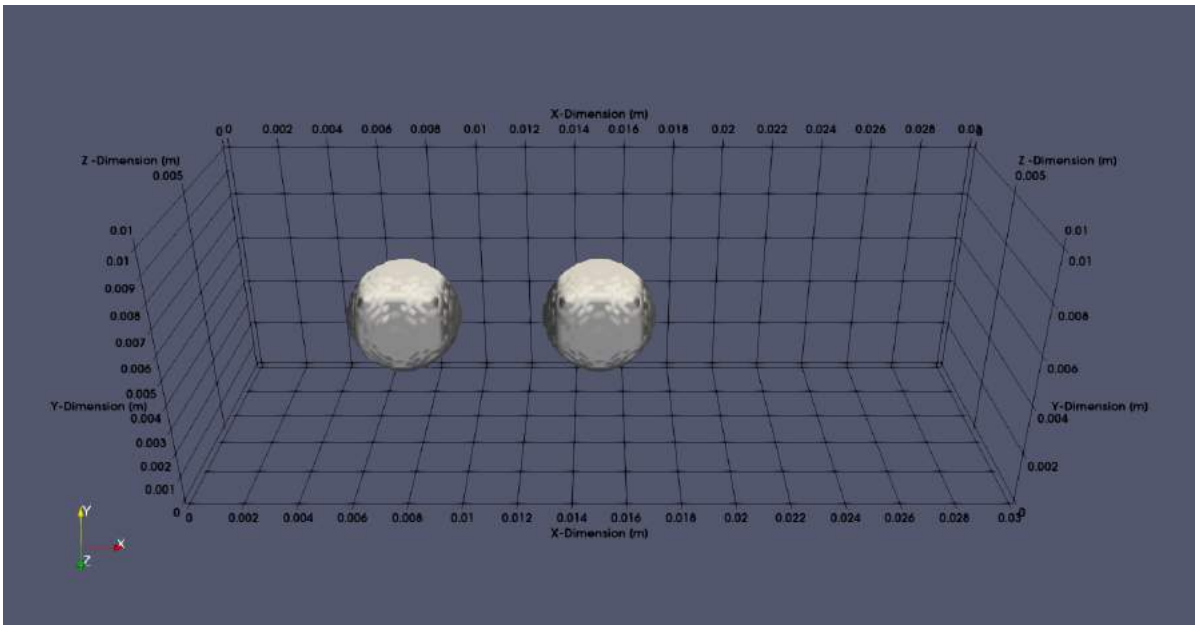

Figure 3: Collision of two spheres in a domain of dimension $0.03m \times 0.01m \times 0.01m$. Both spheres have a radius $R_p = 2 \cdot 10^{-3}m$ and a density $\rho_p = 2500 \frac{kg}{m^3}$. The center of both particles is located at the center of the y,z-plain. The first one with an $x_{p1,0} = 7.5 \cdot 10^{-3}m$ and the second one with an $x_{p2,0} = 15 \cdot 10^{-3}m$.

3.1 Study of the initial setup

Initially, the spheres are of radius $R_p = 2 \cdot 10^{-3}m$ and density $\rho_p = 2500 \frac{kg}{m^3}$. The center of the first sphere is located at $\mathbf{x}_{p1,0} = \left(7.5 \cdot 10^{-3}m,\ 5 \cdot 10^{-3}m,\ 5 \cdot 10^{-3}m\right)$ and has an initial velocity of $\mathbf{u}_{p1,0} = \left(0.3 \frac{m}{s},\ 0 \frac{m}{s},\ 0 \frac{m}{s}\right)$. The second sphere is located at $\mathbf{x}_{p2,0} = \left(15 \cdot 10^{-3}m,\ 5 \cdot 10^{-3}m,\ 5 \cdot 10^{-3}m\right)$ and is at rest. The smoothing parameter was set to $\epsilon = 0.5$. Several parameters were altered to investigate the changes caused by the alteration.
To illustrate the initial collision the simulation with the beforehand mentioned parameters was done and an animation was created with ParaView. The resulting images are depicted in Fig. 4.

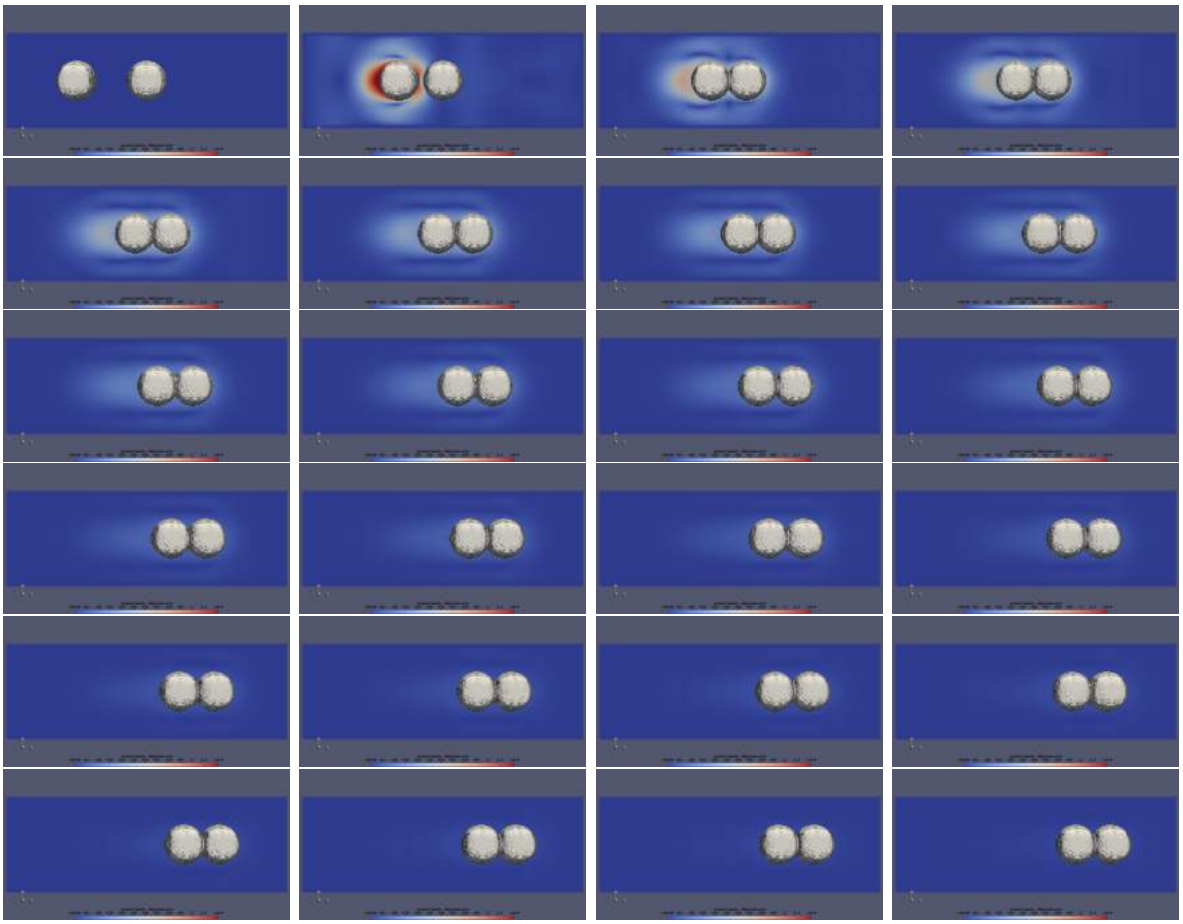

Figure 4: Collision with Initial Parameters: ParaView animation of the collision of two spheres with initial parameters at discrete time steps $\Delta t = 0.02s$. The rectangular slice of the three-dimensional domain shows the magnitude of physical velocity from blue ($0\frac{m}{s}$) to red ($0.12\frac{m}{s}$).

3.1.1 Variation of Epsilon

At first the influence of ϵ_h on the simulation was investigated. As described in Section 2.2 and depicted in Fig. 2, ϵ_h is used to ensure a smooth transition between the solid and fluid regions of the simulation. The violation of momentum conservation in the collision step of pure solid medium is balanced here to conserve the momentum of the whole system. ϵ_h is proportional to spacing h with an arbitrary chosen parameter $\epsilon \geq 0$. To investigate the influence of modifying ϵ the initial state was run with $\epsilon = 0.0, 0.25, 0.5, 0.75, 1.0, 2.0, 3.0, 4.0, 5.0$. The raw data was evaluated and Fig. 5 was created to give a sharp impression of the influence of ϵ. The raw data and information on how the variation was done in the source code is given in the appendix (Section 5).

Fig. 5 shows the velocity (in x-direction) over time plot on the left and the hydrodynamic force over time plot on the right for particle 1 and particle 2. With an increasing value of

ϵ, the velocity decreases and the amount of hydrodynamic force acting on the particles increases for each time step.
In order to simulate solid medium behavior in HLBM accurately, one needs a relative sharp edge of the solid on the one hand, on the other hand a porous transition zone is needed to ensure momentum conservation. The extent of the zone, or more precisely ϵ (with a given spacing h), has to be chosen with care in order to model the particle dimensions right. Is ϵ chosen too large, the transition zone distorts forces acting on the particle and therefore reduces the physical accuracy of the model. With increasing ϵ, the transition zone increases and with it the volume involved in momentum exchange. This influences, among other things, the drag force acting on a particle, result in an over-attenuation of the particle velocity and an increase in the force influencing the particle as seen in Fig. 5. If $\epsilon = 0$ the porous transitioning zone vanishes and physical accuracy of the momentum conservation is in question. To choose the optimal value of ϵ for a given simulation, one needs to compare generated data with references. In general $\epsilon \in (0, 1]$ is a good range to choose from.

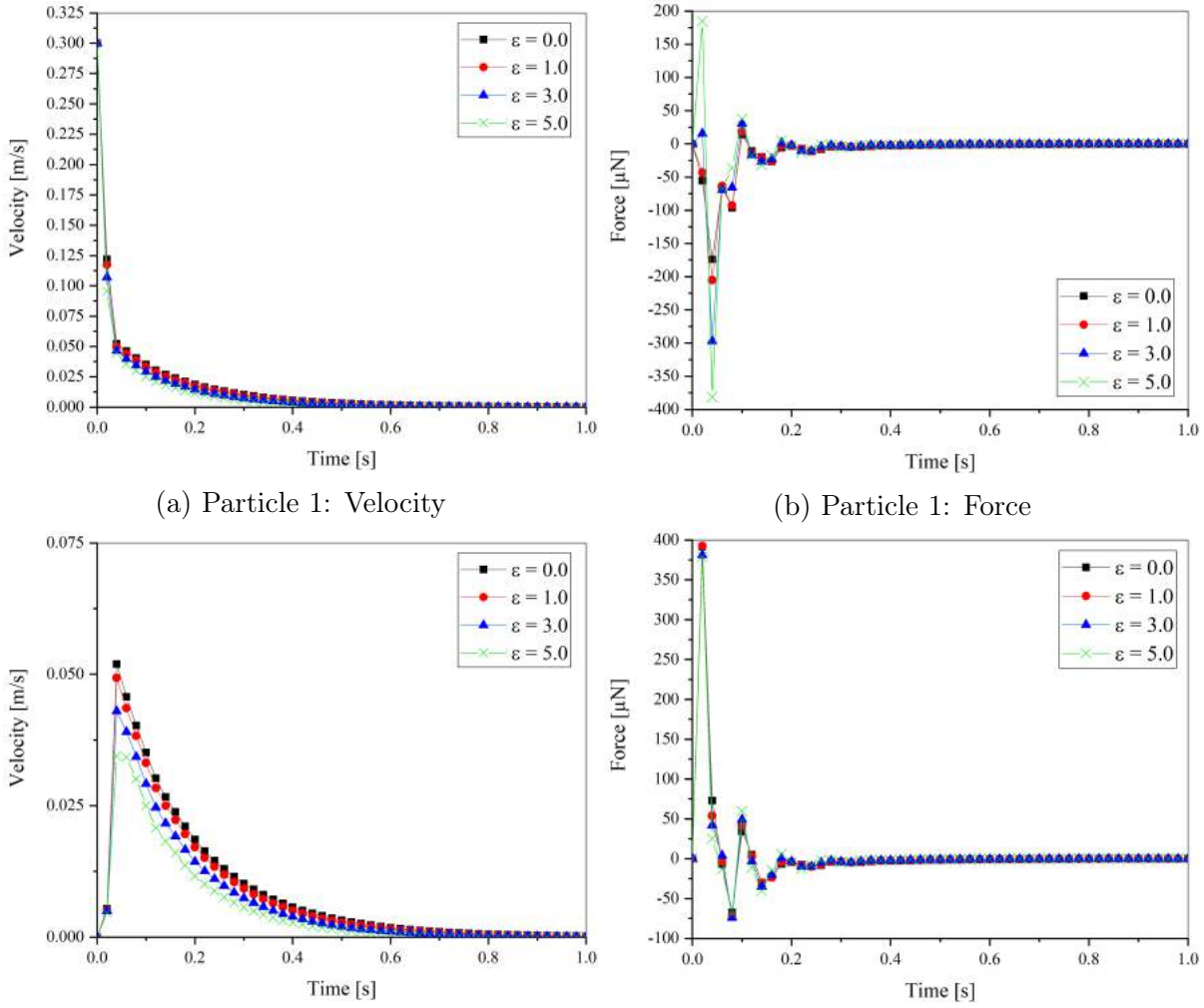

(a) Particle 1: Velocity

(b) Particle 1: Force

(c) Particle 2: Velocity

(d) Particle 2: Force

Figure 5: Variation of Epsilon: plot of velocity in x-direction over time on the left, plot of hydrodynamic force over time on the right for particle 1(a,b) and particle 2(c,d).

3.1.2 Variation of the Particle Density

The density is another point of interest when studying the behavior of particles in a viscous fluid. Materials have a varying density and the difference in density between particle and fluid influences particle-fluid as well as particle-particle interactions.
In the course of this variation the particle density was varied from the density of water (STP) $\rho_f = 1000\frac{kg}{m^3}$, over the density of common window glass $\rho = 2500\frac{kg}{m^3}$, to the density of diamonds $\rho = 3500\frac{kg}{m^3}$ in $500\frac{kg}{m^3}$ increments. Fig. 6 shows the rehashed results. The raw data and information on how the variation was done in the source code is given in the appendix (Section 5).

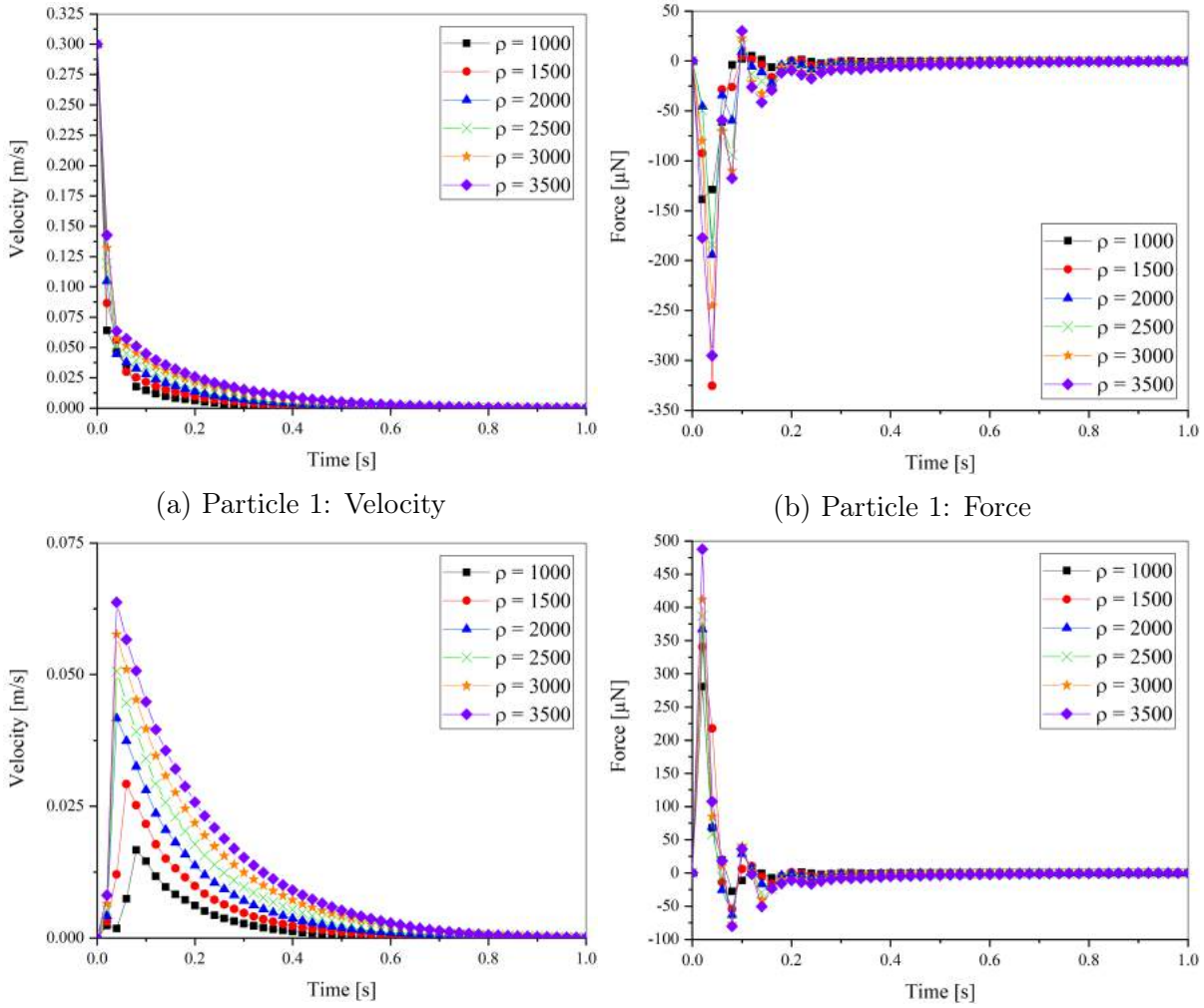

(a) Particle 1: Velocity

(b) Particle 1: Force

(c) Particle 2: Velocity

(d) Particle 2: Force

Figure 6: Variation of Density: plot of velocity in x-direction over time on the left, plot of hydrodynamic force over time on the right for particle 1(a,b) and particle 2(c,d).

Fig. 6 shows the plot of velocity (in x-direction) over time on the left and the plot of

hydrodynamic force over time on the right for particle 1 and particle 2. With increasing density the overall velocity loss over time of particle 1 decreases. The initial velocity increase of particle 2 is on the rise and the velocity loss over time after the third time step decreases. The magnitude of hydrodynamic force acting on a particle increases with an increase in particle density.
The results at hand are in accordance with the preliminary considerations based on the influence of density in the physical behavior of particle-particle and particle-fluid interaction. With an increase in density (and constant volume) the particle mass increases as well. Because the initial particle velocity is set to a constant value of $u_x = 0.3\frac{m}{s}$ this results in an increasing initial momentum held by the first particle. Because the drag force is only dependent on the particle geometry and fluid properties this results in an overall lower velocity loss over time for particle 1. Particle 2 experiences a higher momentum transfer from particle 1, which results in a higher velocity initially after the impact and a flatter decrease of velocity afterwards. The overall hydrodynamic forces acting on the particles increase as well because of the overall higher momentum in the system.

3.1.3 Variation of the Initial Velocity

The last parameter altered for the investigation of the initial setup with one particle in motion and one particle at rest was the initial velocity $\mathbf{u}_{p1,0}$. Fig. 7 shows the particles' velocities $\mathbf{u}_{p1}, \mathbf{u}_{p2}$ and the resulting hydrodynamic forces $\mathbf{F}_{h,p1}, \mathbf{F}_{h,p2}$ as a function of the time. The exact values from the simulation are given in the appendix.
Fig. 7a shows that the velocity of particle 1 decreases as soon as the simulation starts. Accordingly the velocity of the particle which is at rest at $t = 0$ rises (see Fig. 7b). The abrupt change of the gradient is a consequence of the occurring collision. The force plots characteristically show a local maximum for particle 2 and a local minimum for particle 1 respectively before tending towards zero.
As it was pointed out in section 2, the force acting on the particle is directly connected to the motion of the particle through the MEA (see Eq. 19) and the Verlet algorithm (see Eq. 20). Increasing the initial value of the particle velocity $\mathbf{u}_{p,0}$ also leads to higher velocity gradients and increased net momentum in the system (see Eq. 3). Therefore the amplitude in the force-time-diagrams is higher. Furthermore this explains the higher peaks respectively higher maximum velocity values for the second particle. Obviously the increased velocity is also the reason for the decrease of the collision time which utters in a shift of the peaks. Because of the overall smaller gradients the different phases of the collision are best visible in the case $\mathbf{u}_{p1,0} = 0.1\frac{m}{s}$. As shown in Fig. 7a,b particle 1 is decelerated by the fluid while particle 2 is accelerated by the moving fluid before the collision occurs. At approximately $t \approx 0.1s$ the particles collide, which utters in a shift of the gradient. The acceleration of particle 2 increases with the impact, while the deceleration of particle 1 decreases. After that the system tends to the stationary state with passing time.

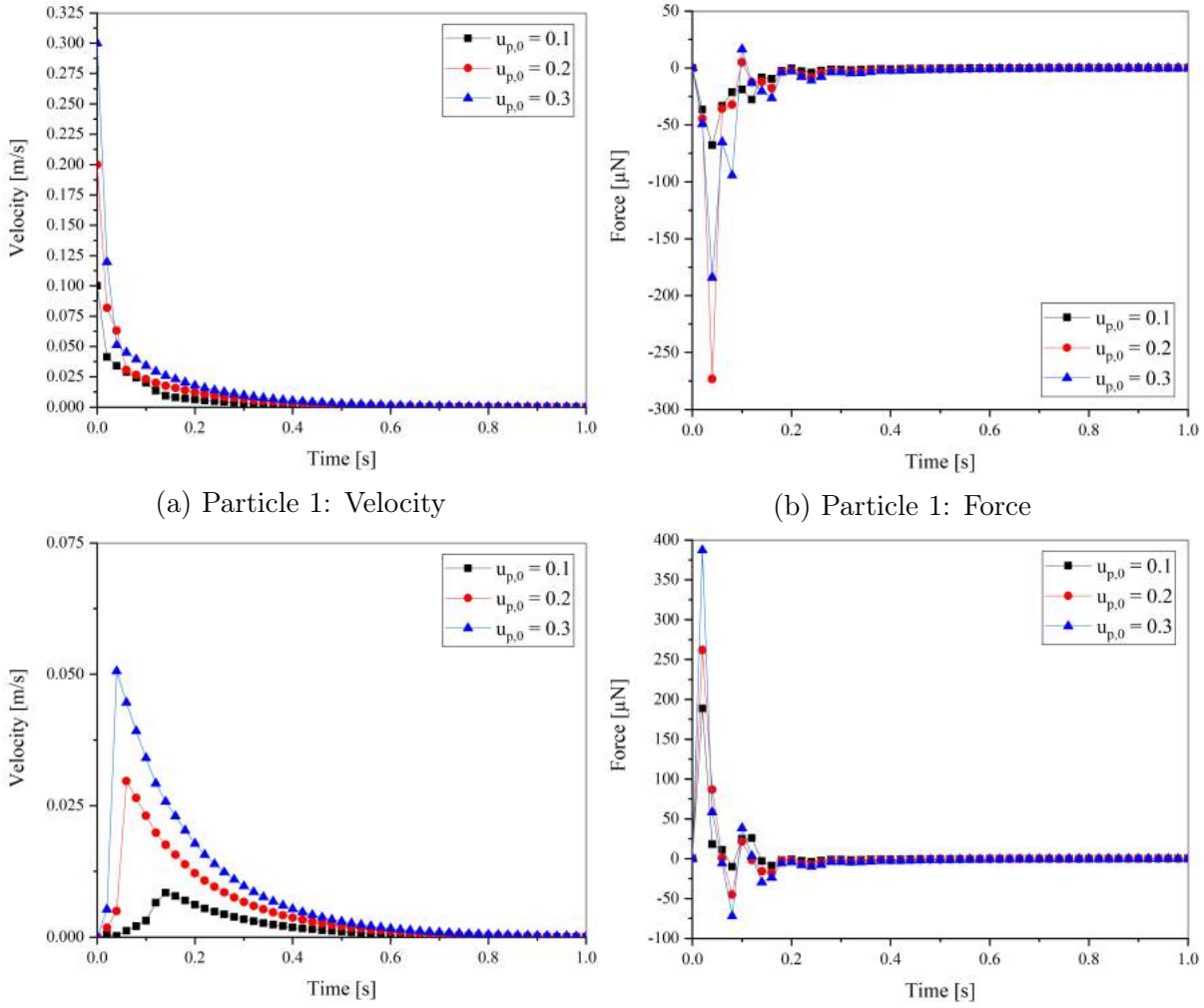

(a) Particle 1: Velocity

(b) Particle 1: Force

(c) Particle 2: Velocity

(d) Particle 2: Force

Figure 7: Variation of initial velocity $\mathbf{u}_{p1,0}$: plot of velocity in x-direction over time on the left, plot of hydrodynamic force over time on the right for particle 1(a,b) and particle 2(c,d).

3.2 Collision with both Spheres in Motion

To study the collision of two spheres further, the initial setup with one particle in motion and one at rest was altered. The position of the second particle was changed from the initial setup to $\mathbf{x}_{p2,0} = \begin{pmatrix} 22, 5 \cdot 10^{-3}m & 5 \cdot 10^{-3}m & 5 \cdot 10^{-3}m \end{pmatrix}$ and given an initial velocity in x-direction $u_{p2,0,x} = -0.3\frac{m}{s}$. In Fig. 8 the animation created with ParaView is shown. The raw data and information on how the variation was done in the source code is given in the appendix (Section 5).

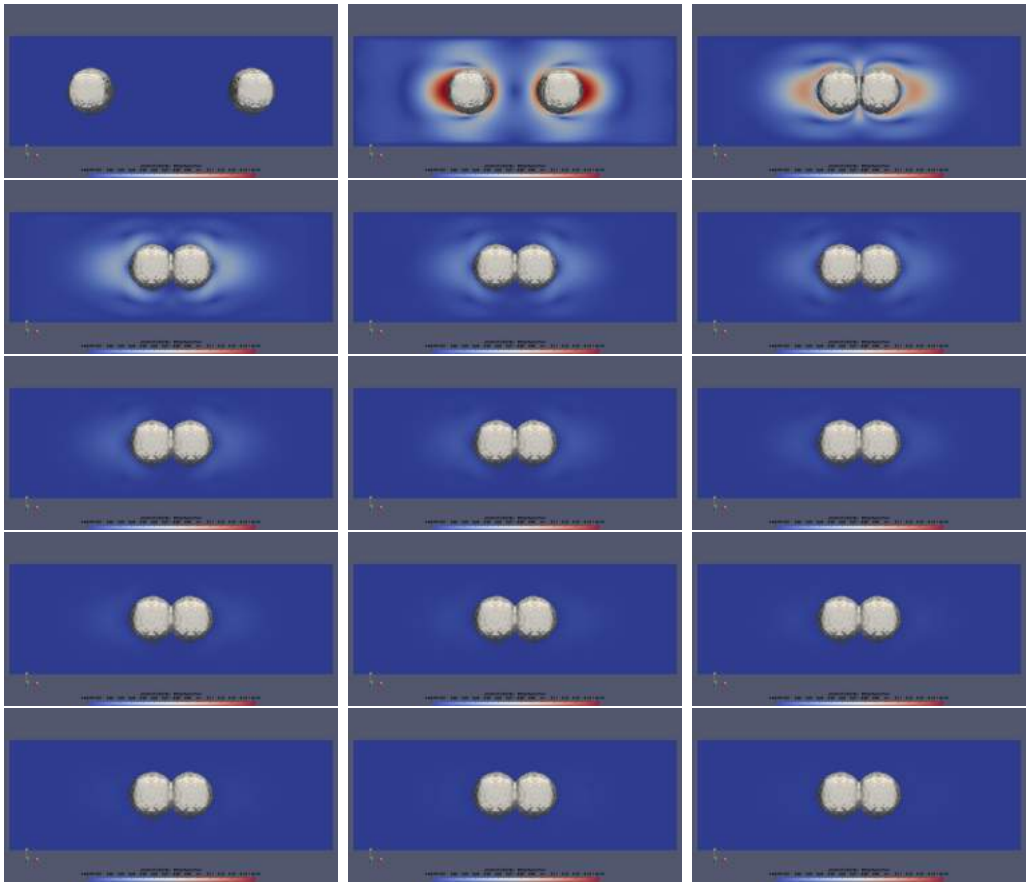

Figure 8: Collision with both Spheres in Motion: ParaView animation of the collision of two spheres with initial parameters at discrete time steps $\Delta t = 0.02s$. The rectangular slice of the three-dimensional domain shows the magnitude of physical velocity from blue ($0\frac{m}{s}$) to red ($0.15\frac{m}{s}$).

Fig. 9 shows the velocity plot for both particles on the left, the hydrodynamic forces involved on the right.

Because the simulation was set up with a mirror symmetry in the center of the domain in all three spacial dimensions, both particles experience the same though mirrored velocity loss through interaction with the fluid. Upon collision both spheres have the same momentum in opposite directions so they come to an abrupt halt. The dissipation

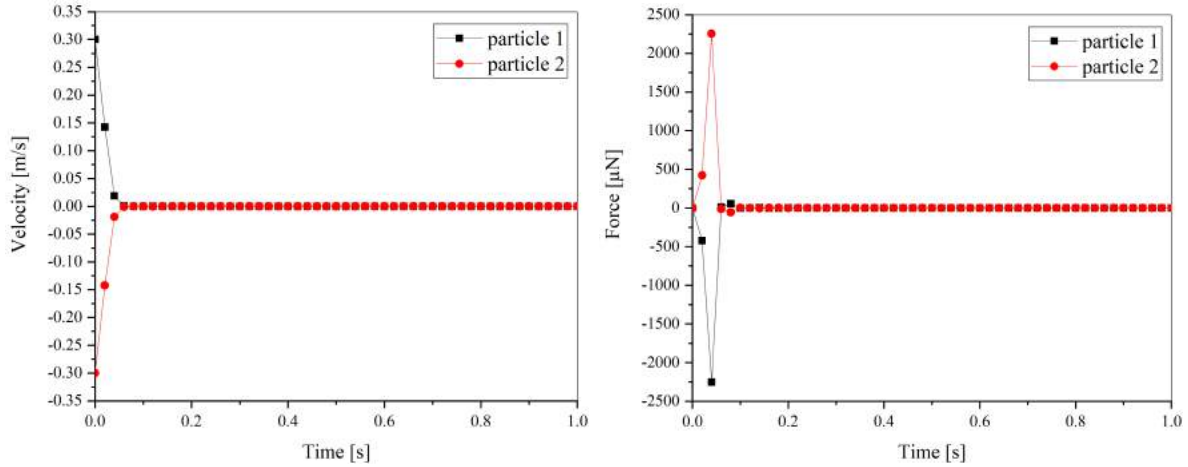

Figure 9: Collision with both spheres in motion: plot of velocity in x-direction over time on the left, plot of hydrodynamic force over time on the right particle 1 and particle 2.

of momentum into the surrounding fluid can be seen in the velocity waves surrounding the particles after collision (Fig. 8).

3.3 Oblique Impact

Apart from the initial setup of a dead center collision of two spheres an oblique impact was simulated to investigate the velocity, effective hydrodynamic forces and the resulting angular velocity. For this purpose the initial position of particle 1 was altered to $\mathbf{x}_{p1,0} = \begin{pmatrix} 7.5 \cdot 10^{-3}m & 3.75 \cdot 10^{-3}m & 5 \cdot 10^{-3}m \end{pmatrix}$, the initial velocity $\mathbf{u}_{p1,0}$ was maintained. Fig. 10 shows an excerpt of the animation generated with the data in ParaView. The raw data, including the whole animation and how the change was implemented in the source code is given in the appendix (Section 5).

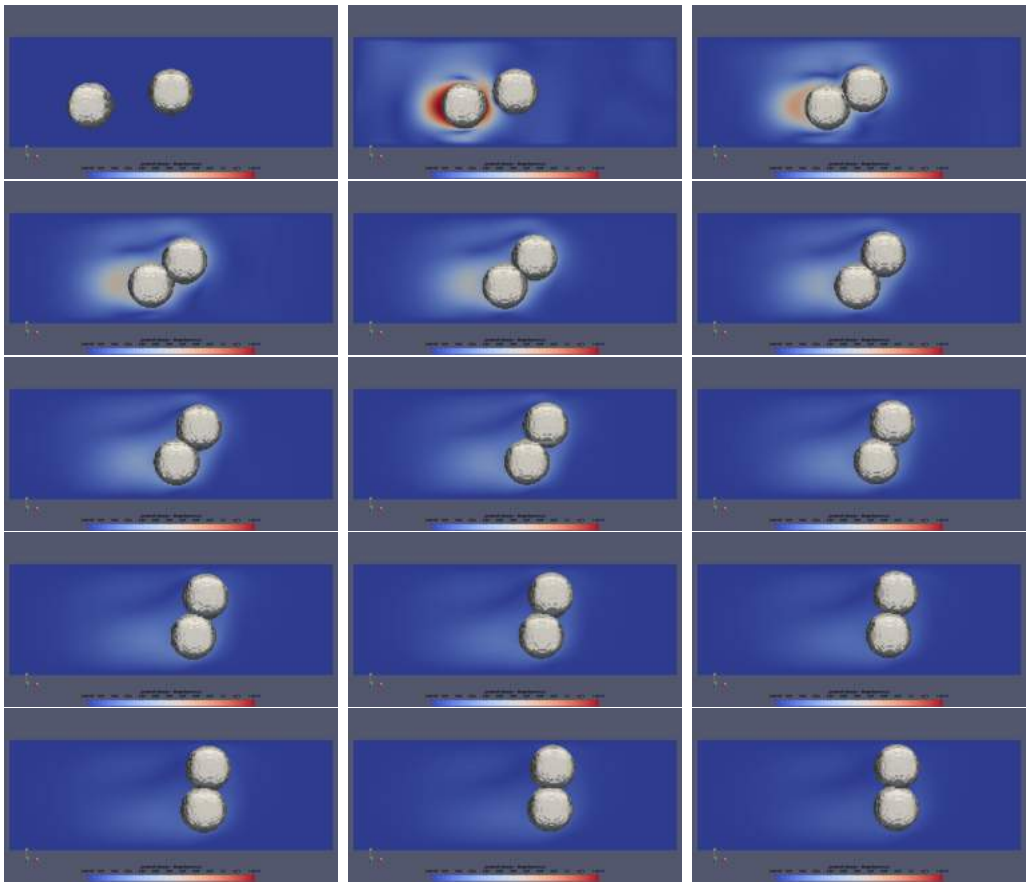

Figure 10: Oblique Collision: Excerpt taken from the ParaView animation of the oblique collision of two spheres. The rectangular slice of the three-dimensional domain shows the magnitude of physical velocity from blue ($0\frac{m}{s}$) to red ($0.12\frac{m}{s}$).

The intention of this variation was to investigate the behavior of the simulation if angular momentum exchange is involved. The dead center collision of the initial setup only involved translational momentum exchange. In Fig. 11 the velocity in x-direction and the angular velocity of the two spheres is depicted as well as the hydrodynamic forces acting on them.

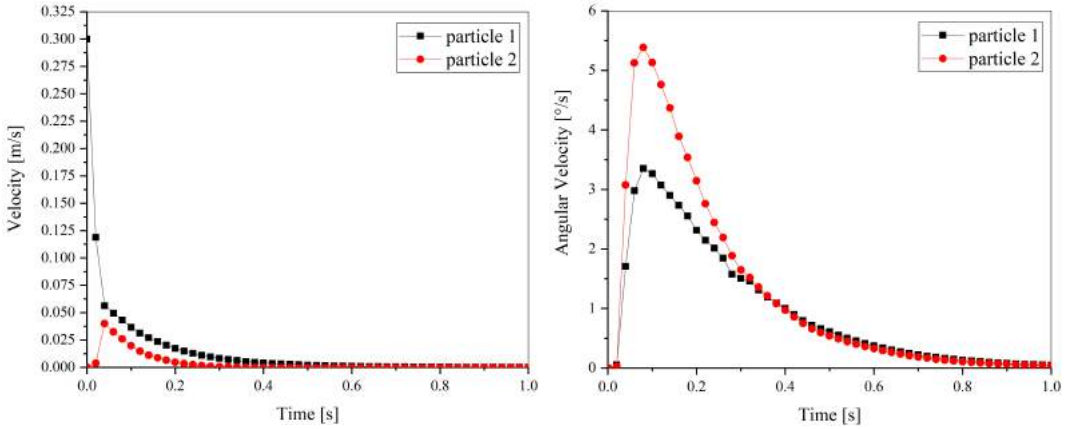

(a) Velocity in x-Direction

(b) Angular Velocity in z-Direction

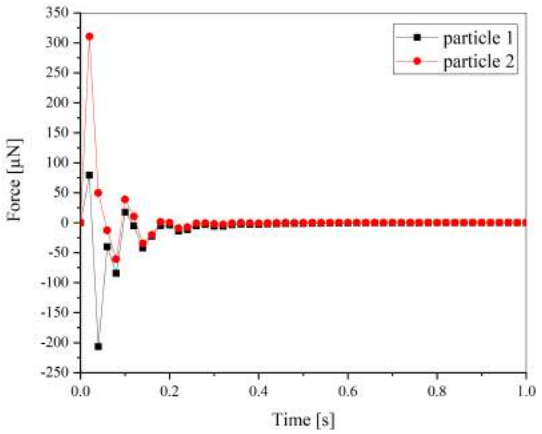

(c) Hydrodynamic Force

Figure 11: Plots of the oblique collision: (a) velocity in x-direction over time, (b) angular velocity in z-direction over time, (c) hydrodynamic force over time.

The velocity of particle 1 decreases in a steep angle in the first three time steps and flattens out after that while approaching zero. While at rest at offset, the velocity of particle 2 increases until the third time step. Then it decreases again and flattens out while approaching zero just as particle 1 does. Both particles pick up angular velocity after the second time step until reaching their peeks at the fifth, then the angular momentum decreases again. As can be seen in the plot for the angular velocity (Fig. 11 (a, right)), the oblique collision leads to an angular momentum exchange. The initial translational momentum of sphere 1 is transferred in part into an angular one and both spheres start spinning after impact. Both types of velocity experience a dampening caused by the viscous fluid and over time both spheres reach a resting state. Because the collision is purely rigid the particles do not bounce off each other, instead they start to spin around each other while in contact. In addition they drift a bit to the right caused by the left over momentum in that direction that was not transferred into angular momentum or dissipated into the fluid.

4 Conclusion

A HLBM approach to simulate the collision of two spheres in a 3D domain is presented. In order to ensure momentum conversion a transitional domain with porous character is implemented to describe the boundary of the particles. In addition to head on collision an oblique impact is investigated to analyze translational motion and angular momentum in the system. The study shows that this approach makes it possible to generate physically plausible results without incorporating an explicit collision model.
There are several interesting aspects for further investigation to explore the great potential of the method. For instance a research on an ideal smoothing parameter ϵ in order to model physical phenomena like lubrication forces is needed. Also introducing the elasticity of solid objects into the model is of interest. Furthermore limitations to the model considering the Reynolds number have to be investigated.

5 Appendix

Extracting Particle Data

In order to be able to plot data of the simulations an output into a data file has to be implemented. The original source code prints the particle data only as a temporary console output. The following code snippet was added to the source code for this purpose:

```
. . .

int main(int argc, char* argv[])
{
. . .

    // Opening data output streams & putting header
    std::ofstream vout("tmp/vel0utput.dat", std::ios::trunc);
    vout << "physTime, velSph1, velSph2, omega1x, omega1y, omega1z,
    omega2x, omega2y, omega2z" << std::endl;
    std::ofstream fout("tmp/force0utput.dat", std::ios::trunc);
    fout << "physTime, forceSph1, forceSph2" << std::endl;
    . . .

    for (int iT = 0; iT < converter.getLatticeTime(maxPhysT)+10; ++iT) {
    particleDynamics.simulateTimestep("verlet");
    getResults(sLattice, converter, iT, superGeometry, timer, particleDynamics);
    sLattice.collideAndStream();
    superExtPorosity.communicate();
    superExtNumerator.communicate();
    superExtDenominator.communicate();

    if (iT % converter.getLatticeTime(iTwrite) == 0) {
    . . .

        //Output format Velocity & Forces:
        //[physTime, valueSphere1, valueSphere2]
        vout << converter.getPhysTime(iT) <<", " << particleIndicator1.getVel()[0] <<", "
        << particleIndicator2.getVel()[0] <<", " << particleIndicator1.getOmega()[0] <<", "
        << particleIndicator1.getOmega()[1] <<", " << particleIndicator1.getOmega()[2] <<", "
        << particleIndicator2.getOmega()[0] <<", " << particleIndicator2.getOmega()[1] <<", "
        << particleIndicator2.getOmega()[2] << std::endl;
        fout << converter.getPhysTime(iT) <<", " << particleIndicator1.getForce()[0] <<", "
        << particleIndicator2.getForce()[0] << std::endl;
    }

  }

. . .
}
```

Variation of Epsilon

Change prefactor of epsilon (here: 0.5) to a value of choice:

```
. . .

    int main(int argc, char* argv[])
{
. . .

// Create Particle Dynamics
  ParticleDynamics3D<T, DESCRIPTOR> particleDynamics(...);

  T epsilon = 0.5*converter.getConversionFactorLength();

. . .
}
```

Velocity (x-Direction)

Time [s]	Velocity in x-Direction [m/s]																	
	Particle 1									Particle 2								
	$\epsilon = 0.0$	$\epsilon = 0.25$	$\epsilon = 0.5$	$\epsilon = 0.75$	$\epsilon = 1.0$	$\epsilon = 2.0$	$\epsilon = 3.0$	$\epsilon = 4.0$	$\epsilon = 5.0$	$\epsilon = 0.0$	$\epsilon = 0.25$	$\epsilon = 0.5$	$\epsilon = 0.75$	$\epsilon = 1.0$	$\epsilon = 2.0$	$\epsilon = 3.0$	$\epsilon = 4.0$	$\epsilon = 5.0$
0	0,3	0,3	0,3	0,3	0,3	0,3	0,3	0,3	0,3	0	0	0	0	0	0	0	0	0
0,02	0,121928	0,120814	0,119686	0,1185	0,117346	0,112558	0,106922	0,101239	0,0955396	0,00538742	0,00529227	0,00524158	0,00520552	0,00518683	0,00509766	0,00495335	0,00480883	0,0046664
0,04	0,052254	0,0516627	0,0511153	0,0505761	0,0501075	0,0483506	0,0465793	0,0454123	0,04457	0,0519107	0,0512105	0,0505917	0,0499523	0,0493194	0,0465765	0,042996	0,0388336	0,0344105
0,06	0,046109	0,0455336	0,0450038	0,0444816	0,0440091	0,0420513	0,0397519	0,0374977	0,0353015	0,0457361	0,0451439	0,0446228	0,0440866	0,0435759	0,0415269	0,0390517	0,0366214	0,0342138
0,08	0,0403979	0,0398325	0,0393423	0,0388614	0,0384205	0,0366235	0,0344474	0,0323018	0,0301811	0,0402519	0,039689	0,0392042	0,0387203	0,0382723	0,0364629	0,0343052	0,0322019	0,0301291
0,1	0,0351185	0,0345721	0,0340919	0,0336042	0,0331632	0,0313703	0,0292184	0,0271101	0,0250423	0,0351167	0,0345533	0,0340665	0,0335935	0,0331479	0,0313384	0,0291831	0,0270722	0,0249977
0,12	0,0303074	0,0297938	0,0293391	0,028885	0,0284762	0,0268006	0,0248094	0,0228696	0,0209782	0,0302431	0,0297013	0,0292422	0,0287931	0,0283669	0,0266664	0,0246437	0,0226833	0,0207747
0,14	0,0267538	0,0262624	0,0258462	0,0254283	0,0250472	0,0235112	0,0216993	0,0199519	0,0182636	0,0266632	0,0261918	0,0257606	0,0253495	0,0249689	0,0234339	0,0216202	0,0198793	0,0182002
0,16	0,0238716	0,0234145	0,0230346	0,0226515	0,0223058	0,0209007	0,0192376	0,0176342	0,0160786	0,0238116	0,0233731	0,0229761	0,0226	0,0222472	0,0208394	0,0191715	0,0175675	0,0160138
0,18	0,0211372	0,020711	0,0203412	0,0199791	0,019644	0,018299	0,016706	0,0151715	0,0136897	0,0210612	0,0206292	0,0202669	0,0199001	0,0195698	0,0182278	0,0166382	0,0151055	0,0136247
0,2	0,0185772	0,0181668	0,0178221	0,0174772	0,0171641	0,0158983	0,0144117	0,0129897	0,0116291	0,0185311	0,0181332	0,0177789	0,0174402	0,0171227	0,0158596	0,0143741	0,012954	0,0115965
0,22	0,0163994	0,0160207	0,0157018	0,0153851	0,0150964	0,0139378	0,0125906	0,0113141	0,0101066	0,0163758	0,0160055	0,0156787	0,0153668	0,0150756	0,0139205	0,0125713	0,0112947	0,0100844
0,24	0,0145809	0,0142308	0,013939	0,0136513	0,0133869	0,0123351	0,0111096	0,00995141	0,00885099	0,014551	0,0142088	0,0139128	0,0136223	0,0133599	0,0123026	0,0110758	0,00991516	0,00881608
0,26	0,0129853	0,0126637	0,0123878	0,0121195	0,0118744	0,0108907	0,00974565	0,00866099	0,00763306	0,0129589	0,0126328	0,0123611	0,0120918	0,0118449	0,0108629	0,00971855	0,00863571	0,00761056
0,28	0,0115213	0,0112157	0,0109603	0,0107085	0,0104774	0,00955657	0,00848981	0,00748619	0,00654554	0,0114996	0,0111986	0,0109408	0,0106874	0,0104597	0,00953961	0,0084751	0,00747374	0,00653495
0,3	0,010203	0,00992222	0,00968535	0,0094512	0,00923815	0,00839007	0,0074171	0,00651224	0,00567339	0,0101935	0,00991262	0,00967223	0,00943997	0,00922734	0,00837982	0,00740781	0,00650287	0,00566335
0,32	0,00906573	0,00880649	0,00858673	0,00837238	0,00817767	0,00740474	0,00652264	0,00570571	0,00494906	0,00905956	0,00879775	0,00857741	0,00836488	0,0081693	0,00739559	0,00651252	0,00569486	0,00493795
0,34	0,0080723	0,0078328	0,00763079	0,00743394	0,00725507	0,0065458	0,00573596	0,00498573	0,00429093	0,00806432	0,00782293	0,00762036	0,00742458	0,00724545	0,0065354	0,00572569	0,00497567	0,00428183
0,36	0,00718654	0,00696504	0,00677807	0,00659566	0,00642983	0,00577266	0,00502524	0,00433505	0,00370144	0,00717923	0,0069562	0,00676838	0,00658616	0,00642149	0,00576466	0,00501771	0,00432887	0,00369658
0,38	0,0063893	0,00618437	0,00601199	0,00584326	0,00568986	0,00508381	0,00439905	0,0037737	0,00320596	0,00638471	0,00617928	0,00600609	0,00583694	0,00568411	0,00507863	0,00439508	0,00377013	0,00320241
0,4	0,00568326	0,00549228	0,0053324	0,00517769	0,0050369	0,00448283	0,00386188	0,00329836	0,00278917	0,00567798	0,00548766	0,00532892	0,00517427	0,00503295	0,00447943	0,00385821	0,00329464	0,00278533
0,42	0,00505776	0,00488282	0,0047363	0,00459425	0,00446563	0,00396009	0,00339521	0,00288397	0,00242237	0,0050542	0,00487921	0,00473263	0,00459058	0,00446252	0,00395642	0,00339151	0,00288009	0,00241882
0,44	0,00450379	0,00434336	0,00420969	0,00407946	0,00396139	0,00349829	0,00298192	0,00251538	0,00209689	0,00450143	0,00434073	0,00420693	0,00407633	0,00395782	0,00349498	0,00297866	0,00251271	0,00209464
0,46	0,00401304	0,00386413	0,00374039	0,00362055	0,00351219	0,00308717	0,00261531	0,00219247	0,00181668	0,00400923	0,00386076	0,00373724	0,00361743	0,00350957	0,00308452	0,00261325	0,00219082	0,00181524
0,48	0,00357189	0,00343558	0,00332214	0,00321228	0,00311269	0,00272378	0,00229252	0,00191431	0,00157807	0,0035699	0,00343359	0,00332035	0,00321048	0,00311064	0,00272218	0,00229382	0,00191229	0,00157669
0,5	0,00318085	0,00305523	0,00295101	0,00285024	0,00275927	0,00240508	0,00201681	0,00167311	0,0013708	0,00317916	0,00305364	0,00294929	0,00284866	0,0027578	0,00240377	0,00201541	0,0016717	0,00136949
0,52	0,00283296	0,00271754	0,00262224	0,0025303	0,00244742	0,00212472	0,0017722	0,00146107	0,00118867	0,00283126	0,00271609	0,00262077	0,00252901	0,00244624	0,00212337	0,0017709	0,00145993	0,00118771
0,54	0,00252265	0,00241788	0,00233101	0,00224698	0,00217106	0,00187659	0,00155612	0,00127487	0,0010305	0,00252198	0,00241692	0,00233003	0,00224597	0,00216983	0,00187546	0,00155516	0,00127411	0,00102985
0,56	0,00224824	0,00215149	0,00207177	0,00199487	0,00192547	0,00165693	0,00136614	0,00111291	0,000894518	0,00224725	0,00215063	0,00207082	0,00199387	0,00192443	0,00165615	0,00136551	0,00111233	0,000893954
0,58	0,00200242	0,00191388	0,00184093	0,00177067	0,00170743	0,00146313	0,00119996	0,000972244	0,000776814	0,00200117	0,00191291	0,00184005	0,00176979	0,00170676	0,00146254	0,00119944	0,000971695	0,000776283
0,6	0,0017837	0,00170253	0,00163589	0,00157187	0,00151437	0,00129234	0,00105438	0,000849275	0,000674071	0,00178295	0,00170184	0,00163519	0,00157127	0,00151386	0,00129183	0,0010539	0,000848801	0,000673658
0,62	0,00158814	0,00151483	0,00145406	0,00139576	0,00134332	0,00114162	0,000926316	0,000741489	0,000584667	0,00158785	0,00151434	0,00145359	0,00139534	0,00134285	0,00114114	0,000925879	0,000741137	0,000584388
0,64	0,00141513	0,00134774	0,00129269	0,0012395	0,00119164	0,00100834	0,000813583	0,000647358	0,000507379	0,00141484	0,0013474	0,00129233	0,00123911	0,00119119	0,00100793	0,000813255	0,000647104	0,000507159
0,66	0,00126101	0,00119935	0,00114896	0,00110053	0,001057	0,000890509	0,000714591	0,000565384	0,000440494	0,0012606	0,00119905	0,00114864	0,0011002	0,00105662	0,000890215	0,000714345	0,000565168	0,000440293
0,68	0,00112334	0,00106711	0,00102111	0,000977076	0,000937518	0,000786522	0,000627767	0,000493862	0,000382328	0,00112282	0,00106675	0,0010208	0,000976771	0,000937209	0,000786287	0,000627551	0,000493666	0,000382162
0,7	0,00100049	0,000949325	0,000907492	0,000867444	0,00083157	0,000694759	0,000551511	0,0004313	0,000331734	0,00100007	0,000949015	0,0009072	0,00086719	0,000831331	0,000694567	0,000551325	0,000431145	0,000331612
0,72	0,000891441	0,000844562	0,000806577	0,000770177	0,000737643	0,000613714	0,000484461	0,000376613	0,000287875	0,000891122	0,00084429	0,00080635	0,000769935	0,00073746	0,000613556	0,000484318	0,000376498	0,000287778
0,74	0,000794092	0,00075148	0,000716876	0,000683828	0,00065439	0,000542094	0,00042554	0,000328896	0,00024988	0,000793926	0,000751272	0,00071669	0,00068363	0,000654192	0,000541969	0,000425433	0,000328806	0,000249796
0,76	0,000707236	0,000668671	0,000637166	0,000607172	0,00058428	0,00047882	0,000373811	0,000287265	0,000216892	0,000707057	0,00066847	0,00063691	0,000607022	0,000580311	0,000478723	0,000373727	0,000287184	0,000216821
0,78	0,000629709	0,000594962	0,000566327	0,000539118	0,00051486	0,000422949	0,000328394	0,000250893	0,000188223	0,00062963	0,000594809	0,000566198	0,000538997	0,000514758	0,000422858	0,000328322	0,000250824	0,000188168
0,8	0,000560915	0,000529333	0,000503378	0,000478691	0,00045696	0,000373601	0,000288491	0,000219104	0,000163344	0,000560824	0,000529229	0,000503276	0,000478602	0,000456611	0,000373524	0,0002884	0,00021905	0,000163299
0,82	0,000499767	0,000470921	0,000447446	0,000425053	0,00040514	0,000330007	0,000253425	0,000191344	0,000141771	0,000499667	0,000470839	0,000447366	0,000424981	0,00040503	0,000329943	0,000253374	0,0001913	0,000141733
0,84	0,000445225	0,000418963	0,00039774	0,00037743	0,00035937	0,00029149	0,000222621	0,000167112	0,00012352	0,000445177	0,000418891	0,000397676	0,000377365	0,00035927	0,000291438	0,000222579	0,000167075	0,000123019
0,86	0,000396664	0,000372741	0,000353548	0,000335135	0,00031873	0,000257467	0,000195567	0,000145951	0,000106794	0,000396613	0,000372689	0,000353498	0,000335082	0,000318679	0,000257425	0,000195533	0,00014592	0,000106768
0,88	0,000353385	0,000331633	0,000314252	0,000297574	0,00028271	0,000227417	0,000171803	0,00012763	9,27E-05	0,000353324	0,000331592	0,00031429	0,000297531	0,000282672	0,000227382	0,000171775	0,000127439	9,27E-05
0,9	0,000314792	0,000295065	0,000279309	0,00026422	0,00025073	0,000200873	0,000150925	0,000111315	8,04E-05	0,00031474	0,000295033	0,000279272	0,000264182	0,000250734	0,000200847	0,000150901	0,000111296	8,04E-05
0,92	0,000280356	0,000262532	0,000248243	0,0002346	0,00022243	0,000177428	0,000132581	9,72E-05	6,98E-05	0,00028031	0,000262502	0,00024821	0,00023456	0,00022402	0,000177406	0,000132562	9,72E-05	6,98E-05
0,94	0,000249656	0,00023358	0,000220627	0,000208298	0,00019730	0,000156717	0,000116468	8,49E-05	6,06E-05	0,00024961	0,000233553	0,0002206	0,000208266	0,000197274	0,000156699	0,000116452	8,49E-05	6,06E-05
0,96	0,000222389	0,000207816	0,000196082	0,00018494	0,00017501	0,000138423	0,000102314	7,41E-05	5,26E-05	0,00022245	0,00020779	0,00019605	0,00018491	0,00017498	0,00013840	0,000102301	7,41E-05	5,26E-05
0,98	0,000198076	0,000184887	0,000174265	0,000164198	0,00015523	0,000122267	8,99E-05	6,48E-05	4,56E-05	0,000198029	0,000184862	0,00017424	0,000164176	0,000155211	0,00012225	8,99E-05	6,47E-05	4,56E-05
1	0,000176473	0,000164484	0,000154876	0,000145782	0,000137694	0,000107995	7,90E-05	5,66E-05	3,96E-05	0,000176428	0,000164461	0,000154854	0,000145763	0,000137671	0,00010798	7,89E-05	5,65E-05	3,96E-05

Hydrodynamic Force

Time [s]	Hydrodynamic Force [μN]																		
	Particle 1									Particle 2									
	$\epsilon = 0.0$	$\epsilon = 0.25$	$\epsilon = 0.5$	$\epsilon = 0.75$	$\epsilon = 1.0$	$\epsilon = 2.0$	$\epsilon = 3.0$	$\epsilon = 4.0$	$\epsilon = 5.0$	$\epsilon = 0.0$	$\epsilon = 0.25$	$\epsilon = 0.5$	$\epsilon = 0.75$	$\epsilon = 1.0$	$\epsilon = 2.0$	$\epsilon = 3.0$	$\epsilon = 4.0$	$\epsilon = 5.0$
0	0	0	0	0	0	0	0	0	0	0	0	0	0	0	0	0	0	0	0
0,02	-55,1022	-58,4685	-49,2104	-45,5878	-43,1691	-30,3645	15,3669	91,8476	184,556	391,505	380,491	387,055	391,007	392,67	388,505	381,367	377,314	378,525	
0,04	-174,017	-182,971	-184,239	-193,477	-205,502	-249,844	-297,044	-350,287	-381,323	72,7009	70	58,2756	54,1147	53,8419	46,9188	41,7799	36,5475	25,2546	
0,06	-65,6141	-65,3828	-65,105	-64,7715	-63,5473	-64,1663	-69,2882	-68,5336	-67,2659	-6,88616	-7,33703	-5,75753	-4,08535	-3,7228	2,14426	3,95524	-0,592439	-13,2238	
0,08	-96,0796	-94,5181	-94,1545	-94,5382	-92,9099	-81,978	-65,5172	-49,7567	-36,4843	-67,861	-71,3042	-71,9554	-71,0935	-71,8094	-73,9358	-74,1505	-73,6781	-69,5513	
0,1	14,0952	14,3741	16,4061	18,0298	18,6902	23,6023	30,1161	35,4771	37,7205	34,2544	37,5442	38,2776	39,8557	41,7581	46,5832	49,1781	54,1783	59,4651	
0,12	-10,6889	-12,5635	-13,0662	-14,0121	-14,4371	-16,3649	-16,8589	-17,0904	-17,235	4,99258	4,0765	3,4916	3,27681	2,89122	0,492221	-3,28679	-7,56822	-11,2714	
0,14	-19,9143	-19,7126	-20,3909	-20,4731	-21,2254	-23,6496	-26,4403	-29,1056	-31,7442	-30,2411	-29,861	-29,5931	-30,259	-30,2544	-32,2782	-35,1489	-38,1664	-40,393	
0,16	-26,7926	-26,1392	-26,4481	-26,3024	-26,3557	-25,4171	-23,2648	-20,3936	-17,2209	-23,4322	-23,8907	-23,9175	-23,9237	-23,4213	-22,3089	-20,437	-17,6473	-14,2674	
0,18	-5,65665	-4,99869	-4,02231	-3,51048	-2,89168	-0,556654	1,52735	3,43079	5,18553	-6,56511	-6,11026	-5,7773	-4,8142	-4,48095	-2,06266	0,783114	3,305	5,43023	
0,2	-3,21022	-3,08277	-2,98703	-2,9192	-2,71545	-2,26923	-1,97068	-1,96185	-2,46705	-4,59118	-4,2215	-4,24295	-3,94881	-3,89802	-3,56603	-3,44692	-3,73467	-4,33282	
0,22	-7,3793	-7,33059	-7,61035	-7,85425	-7,98787	-8,97596	-10,4467	-11,9918	-13,2959	-7,49994	-7,75726	-8,04155	-8,11567	-8,38968	-9,15436	-10,0863	-11,1331	-12,1001	
0,24	-11,5457	-10,9732	-10,9427	-11,074	-11,081	-11,1797	-10,6991	-9,7209	-8,36207	-9,76783	-9,85429	-10,0712	-9,87103	-10,0002	-9,96965	-9,69883	-9,04638	-7,93707	
0,26	-8,30253	-8,00586	-7,73461	-7,42465	-7,18955	-5,93857	-4,35166	-2,80144	-1,34332	-8,2902	-7,8753	-7,66561	-7,56304	-7,28096	-6,31621	-4,90856	-3,34759	-1,86287	
0,28	-4,43008	-4,02883	-3,7802	-3,60344	-3,42354	-2,69511	-2,07145	-1,75336	-1,80397	-4,21314	-4,1626	-4,06347	-3,80059	-3,63004	-2,94511	-2,34822	-2,01947	-1,99987	
0,3	-3,83928	-3,69806	-3,68988	-3,66937	-3,63212	-3,71835	-4,03792	-4,53607	-4,9943	-3,92288	-4,03621	-3,92282	-3,83099	-3,85266	-3,83911	-4,00148	-4,33878	-4,70679	
0,32	-4,74094	-4,73025	-4,77813	-4,82193	-4,8543	-4,99297	-5,01895	-4,79434	-4,29684	-4,57875	-4,71267	-4,69904	-4,68607	-4,74025	-4,83099	-4,79978	-4,61849	-4,1801	
0,34	-4,63911	-4,62232	-4,58026	-4,51039	-4,43578	-4,08395	-3,47831	-2,71147	-1,91512	-4,67327	-4,45814	-4,38149	-4,29586	-4,27484	-3,95879	-3,40436	-2,7171	-1,98289	
0,36	-3,69325	-3,60644	-3,49177	-3,36204	-3,23223	-2,70368	-2,10891	-1,64853	-1,40405	-3,65812	-3,61427	-3,47629	-3,34627	-3,25794	-2,76881	-2,22338	-1,77663	-1,50517	
0,38	-2,76862	-2,69221	-2,60652	-2,52583	-2,45189	-2,20682	-2,05887	-2,07335	-2,15764	-2,86895	-2,75089	-2,69943	-2,6182	-2,52857	-2,29134	-2,11984	-2,07806	-2,11717	
0,4	-2,54689	-2,5068	-2,46108	-2,43424	-2,41862	-2,37781	-2,36211	-2,30283	-2,12713	-2,60099	-2,53708	-2,48755	-2,4716	-2,43679	-2,35707	-2,29967	-2,22415	-2,05627	
0,42	-2,46843	-2,50545	-2,48443	-2,46237	-2,43864	-2,33141	-2,10675	-1,77813	-1,38535	-2,51992	-2,48868	-2,45311	-2,41539	-2,3969	-2,27693	-2,06172	-1,75977	-1,39519	
0,44	-2,34483	-2,28006	-2,22655	-2,17933	-2,12755	-1,88923	-1,55659	-1,23464	-0,991684	-2,34059	-2,23752	-2,19213	-2,14441	-2,09668	-1,87515	-1,57093	-1,26798	-1,02749	
0,46	-1,9864	-1,91785	-1,85594	-1,7922	-1,73128	-1,50019	-1,27386	-1,13466	-1,07302	-1,94463	-1,92365	-1,85454	-1,79197	-1,74234	-1,52449	-1,29898	-1,14834	-1,06877	
0,48	-1,68974	-1,62288	-1,56528	-1,5229	-1,48424	-1,35005	-1,24437	-1,17064	-1,07512	-1,67256	-1,6283	-1,57883	-1,54106	-1,50184	-1,36167	-1,24223	-1,15407	-1,05336	
0,5	-1,4998	-1,46051	-1,43038	-1,40168	-1,3766	-1,28682	-1,17413	-1,0284	-0,840957	-1,50404	-1,47431	-1,44027	-1,40702	-1,37497	-1,27628	-1,15752	-1,01447	-0,836887	
0,52	-1,41715	-1,35258	-1,324	-1,29552	-1,27081	-1,1566	-0,988872	-0,803934	-0,63749	-1,38142	-1,34364	-1,31666	-1,28577	-1,26058	-1,14489	-0,983898	-0,808001	-0,64749	
0,54	-1,26445	-1,2124	-1,17617	-1,14277	-1,11274	-0,976062	-0,812083	-0,677392	-0,587661	-1,22833	-1,20485	-1,16763	-1,13849	-1,10722	-0,975879	-0,818333	-0,684671	-0,590024	
0,56	-1,09154	-1,05423	-1,02264	-0,988645	-0,957328	-0,836459	-0,719112	-0,635537	-0,56412	-1,10451	-1,05566	-1,0232	-0,99	-0,959205	-0,841283	-0,723291	-0,633676	-0,558156	
0,58	-0,966243	-0,92533	-0,895361	-0,86756	-0,842305	-0,752368	-0,663172	-0,577638	-0,479896	-0,975383	-0,930306	-0,897297	-0,870699	-0,8449	-0,753946	-0,660251	-0,572704	-0,476798	
0,6	-0,858966	-0,825848	-0,802732	-0,77986	-0,759692	-0,682687	-0,58775	-0,48591	-0,385829	-0,86	-0,82724	-0,803234	-0,779544	-0,759627	-0,679534	-0,584255	-0,485156	-0,387993	
0,62	-0,769774	-0,745833	-0,722379	-0,701475	-0,682835	-0,601846	-0,501227	-0,408058	-0,334935	-0,773239	-0,743395	-0,720545	-0,699284	-0,680624	-0,600115	-0,501487	-0,410076	-0,336396	
0,64	-0,689515	-0,664542	-0,642572	-0,621405	-0,601888	-0,521867	-0,433155	-0,362339	-0,306919	-0,684831	-0,66268	-0,641133	-0,620252	-0,600785	-0,522295	-0,434635	-0,363137	-0,305702	
0,66	-0,614168	-0,586737	-0,567074	-0,546843	-0,528365	-0,457921	-0,38642	-0,32652	-0,268967	-0,612517	-0,586789	-0,566986	-0,546997	-0,528606	-0,458757	-0,386252	-0,325187	-0,267655	
0,68	-0,539486	-0,51988	-0,501796	-0,483965	-0,46801	-0,408381	-0,344759	-0,2841	-0,225149	-0,540825	-0,520657	-0,502479	-0,484503	-0,468362	-0,408169	-0,343929	-0,283283	-0,22534	
0,7	-0,483976	-0,463961	-0,447195	-0,431846	-0,417733	-0,363636	-0,301455	-0,242575	-0,192626	-0,467937	-0,464403	-0,447122	-0,431826	-0,417388	-0,362831	-0,30092	-0,242869	-0,193173	
0,72	-0,431029	-0,413806	-0,399374	-0,385099	-0,371988	-0,320174	-0,26148	-0,211115	-0,171113	-0,430796	-0,413304	-0,398939	-0,384538	-0,371304	-0,319785	-0,261696	-0,211446	-0,17095	
0,74	-0,384573	-0,368562	-0,355013	-0,341421	-0,32906	-0,28087	-0,22949	-0,187132	-0,150631	-0,383878	-0,368174	-0,354623	-0,341012	-0,328835	-0,280972	-0,229685	-0,186922	-0,150189	
0,76	-0,345589	-0,327185	-0,314473	-0,302012	-0,290854	-0,247921	-0,203263	-0,16444	-0,12898	-0,343848	-0,327063	-0,31431	-0,301928	-0,2909	-0,248046	-0,203088	-0,164106	-0,128897	
0,78	-0,305831	-0,290707	-0,279011	-0,267882	-0,257959	-0,219952	-0,179141	-0,142373	-0,110514	-0,301455	-0,290602	-0,278971	-0,267891	-0,258021	-0,219833	-0,178914	-0,14233	-0,110656	
0,8	-0,272643	-0,258967	-0,248218	-0,238253	-0,229392	-0,194915	-0,156601	-0,123499	-0,0966073	-0,271745	-0,258851	-0,24816	-0,238179	-0,229308	-0,194331	-0,156677	-0,123645	-0,0966119	
0,82	-0,241636	-0,230756	-0,220972	-0,21185	-0,203717	-0,171622	-0,1371	-0,108345	-0,0847222	-0,241278	-0,23067	-0,220737	-0,211723	-0,20365	-0,171641	-0,137152	-0,108335	-0,0845939	
0,84	-0,215837	-0,205338	-0,19638	-0,188035	-0,180555	-0,1513	-0,120654	-0,0951644	-0,0733056	-0,215657	-0,205246	-0,196272	-0,187954	-0,180512	-0,151309	-0,120648	-0,0950638	-0,0732408	
0,86	-0,192072	-0,182507	-0,174442	-0,166784	-0,15998	-0,133694	-0,10633	-0,0829889	-0,0631179	-0,191966	-0,18246	-0,174398	-0,166759	-0,15994	-0,133691	-0,106259	-0,0829316	-0,0631409	
0,88	-0,171169	-0,162224	-0,155029	-0,148068	-0,14189	-0,118283	-0,0933938	-0,0721625	-0,0548151	-0,170769	-0,162199	-0,155028	-0,14806	-0,141885	-0,118252	-0,0933412	-0,0721714	-0,0548254	
0,9	-0,152518	-0,144342	-0,137899	-0,131511	-0,125962	-0,104535	-0,0818608	-0,0630156	-0,0478469	-0,152643	-0,144327	-0,137882	-0,131615	-0,125931	-0,104486	-0,0818552	-0,0630222	-0,0478172	
0,92	-0,135868	-0,128491	-0,12266	-0,116905	-0,111775	-0,0922497	-0,0718657	-0,0551997	-0,0415554	-0,135643	-0,128482	-0,12263	-0,11687	-0,11174	-0,0922303	-0,0718689	-0,0551762	-0,0415255	
0,94	-0,121177	-0,114375	-0,109034	-0,103795	-0,0991126	-0,0814276	-0,0632144	-0,0482507	-0,035924	-0,121431	-0,114356	-0,109006	-0,10377	-0,099089	-0,0814264	-0,0632002	-0,0482251	-0,0359215	
0,96	-0,108277	-0,101762	-0,0968758	-0,0921295	-0,0878809	-0,0719532	-0,0555823	-0,0420614	-0,03114	-0,107954	-0,101755	-0,0968653	-0,0921162	-0,0878693	-0,0719387	-0,055561	-0,0420546	-0,031143	
0,98	-0,0960651	-0,0905369	-0,0860862	-0,0817971	-0,0779581	-0,0635949	-0,0487994	-0,0366936	-0,0270955	-0,0959898	-0,0905351	-0,0860753	-0,0817899	-0,0779456	-0,0635754	-0,0487884	-0,0366948	-0,0270871	
1	-0,0854062	-0,0805604	-0,0765145	-0,0726447	-0,0691723	-0,056171	-0,0428358	-0,0320758	-0,0235482	-0,0854361	-0,0805532	-0,0765142	-0,0726334	-0,0691572	-0,0561573	-0,0428324	-0,032076	-0,0235367	

Variation of Sphere Density

Change constant sphereDensity (here: 2500) to a value of choice:

```
. . .

//Particle Settings
T centerX = 0.0075;
T centerY = lengthY*.5;
T centerZ = lengthZ*.5;
T const sphereDensity = 2500;
T const sphereRadius = 0.002;
Vector<T,3> sphereCenter = {centerX,centerY,centerZ};
Vector<T,3> sphereVelocity = {0.3,0.,0.};
Vector<T,3> externalAcceleration = {0., 0., 0.};

. . .
```

Velocity (x-Direction)

Time [s]	Velocity x-Direction [m/s]											
	Particle 1						Particle 2					
	$\rho = 1000$	$\rho = 1500$	$\rho = 2000$	$\rho = 2500$	$\rho = 3000$	$\rho = 3500$	$\rho = 1000$	$\rho = 1500$	$\rho = 2000$	$\rho = 2500$	$\rho = 3000$	$\rho = 3500$
0	0,3	0,3	0,3	0,3	0,3	0,3	0	0	0	0	0	0
0,02	0,0640684	0,0865349	0,104664	0,119686	0,132235	0,142529	0,00235837	0,00311916	0,00413279	0,00524158	0,00647667	0,0081048
0,04	0,0463001	0,0563985	0,044576	0,0511153	0,0576509	0,0635079	0,00180006	0,0120737	0,0416997	0,0505917	0,0576465	0,0636867
0,06	0,0334485	0,0298241	0,0378168	0,0450038	0,0514572	0,0572057	0,0074293	0,0292214	0,037413	0,0446228	0,0509506	0,056634
0,08	0,0176061	0,0253085	0,032638	0,0393423	0,0454375	0,0509588	0,0167321	0,0251996	0,0325608	0,0392042	0,0452215	0,0507043
0,1	0,0146234	0,0215126	0,0280202	0,0340919	0,0397251	0,0449705	0,0146016	0,0216164	0,0280587	0,0340665	0,0396655	0,0448554
0,12	0,0119302	0,0178474	0,0237031	0,0293391	0,0346794	0,039693	0,0117217	0,0177466	0,0236167	0,0292422	0,0345624	0,0395533
0,14	0,00977729	0,0151781	0,0205835	0,0258462	0,0308953	0,0356831	0,00967599	0,0150813	0,020496	0,0257606	0,0308075	0,0355839
0,16	0,00828584	0,0132136	0,0181785	0,0230346	0,0277169	0,0321968	0,00825887	0,0131979	0,0181451	0,0229761	0,0276394	0,0320879
0,18	0,00723487	0,0115597	0,0159518	0,0203412	0,0246575	0,0288477	0,00721397	0,0115183	0,0158921	0,0202669	0,0245619	0,0287558
0,2	0,00615927	0,00986819	0,0137924	0,0178221	0,021856	0,0258286	0,00612646	0,0098377	0,0137557	0,0177789	0,0218192	0,0257824
0,22	0,00512451	0,00839302	0,0119728	0,0157018	0,0194638	0,0231889	0,00510151	0,00837788	0,0119545	0,0156787	0,0194327	0,0231509
0,24	0,00428361	0,00724804	0,0105165	0,013939	0,0174243	0,0209152	0,00427398	0,0072412	0,0105028	0,0139128	0,017394	0,0208773
0,26	0,00368405	0,00633508	0,00926924	0,0123878	0,0156105	0,0188701	0,00366965	0,00632083	0,00924799	0,0123611	0,0155792	0,0188265
0,28	0,00317966	0,00549604	0,00811433	0,0109603	0,0139441	0,0169938	0,00317201	0,00548144	0,00809905	0,0109408	0,0139177	0,0169595
0,3	0,00270602	0,0047187	0,00707687	0,00968535	0,0124555	0,0153056	0,00269936	0,00471193	0,00706868	0,00967223	0,0124405	0,015282
0,32	0,00227451	0,00406019	0,00619716	0,00858673	0,0111464	0,0137928	0,00226865	0,00405509	0,00619212	0,00857741	0,0111338	0,0137766
0,34	0,00192427	0,00352464	0,00545257	0,00763079	0,00998922	0,0124428	0,00192091	0,00352111	0,00544568	0,00762036	0,00997862	0,0124253
0,36	0,00165041	0,00306804	0,00479412	0,00677807	0,00895398	0,0112197	0,00164801	0,00306274	0,0047875	0,00676838	0,0089438	0,0112024
0,38	0,00141799	0,00265525	0,00420139	0,00601199	0,00801967	0,0101083	0,00141551	0,00265204	0,00419701	0,00600609	0,00801172	0,0100894
0,4	0,00120645	0,00228986	0,00368155	0,0053324	0,0071829	0,00909487	0,00120391	0,00228786	0,00367888	0,00532892	0,00717757	0,00907864
0,42	0,00102034	0,00198074	0,00323257	0,0047363	0,00643696	0,00817442	0,00101855	0,00197891	0,00323045	0,00473263	0,00643214	0,00815925
0,44	0,000867466	0,00172001	0,00284309	0,00420969	0,00577162	0,00733872	0,00086631	0,00171844	0,00284106	0,00420693	0,00576591	0,00732205
0,46	0,000742788	0,00149308	0,00249794	0,00374039	0,00517407	0,00657712	0,000741958	0,00149185	0,00249582	0,00373724	0,00516935	0,00655895
0,48	0,000635595	0,00129218	0,00219192	0,00332214	0,00463671	0,0058792	0,000634974	0,00129137	0,00219049	0,00332035	0,00463308	0,00586349
0,5	0,000540705	0,00111737	0,00192447	0,00295101	0,00415561	0,00524297	0,000540249	0,0011168	0,00192366	0,00294929	0,00415203	0,00522748
0,52	0,000458941	0,000968255	0,00169131	0,00262224	0,00372341	0,00466634	0,000458611	0,000967778	0,00169059	0,00262077	0,00372087	0,00464734
0,54	0,000390982	0,000840305	0,00148662	0,00233101	0,00333708	0,00413591	0,000390724	0,000839693	0,00148583	0,00233003	0,00333443	0,00412019
0,56	0,000334309	0,000728596	0,00130597	0,00207177	0,00299003	0,00365942	0,000334086	0,000728048	0,00130524	0,00207082	0,00298756	0,00364018
0,58	0,00028554	0,000630825	0,00114686	0,00184093	0,00267841	0,00322149	0,000285346	0,000630447	0,00114639	0,00184005	0,00267666	0,00320591
0,6	0,000243061	0,000546239	0,00100754	0,00163589	0,00239947	0,00282934	0,000242905	0,000546011	0,00100725	0,00163519	0,00239754	0,00281285
0,62	0,000206749	0,000473536	0,000885577	0,00145406	0,00214894	0,00247574	0,000206627	0,000473371	0,000885315	0,00145359	0,00214705	0,00245835
0,64	0,000176277	0,000410686	0,000778387	0,00129269	0,00192419	0,00215505	0,000176178	0,000410544	0,000778157	0,00129233	0,00192283	0,00214105
0,66	0,000150564	0,000355945	0,000683956	0,00114896	0,00172293	0,00187024	0,000150473	0,000355835	0,000683764	0,00114864	0,00172175	0,00185683
0,68	0,00012847	0,000308325	0,000600937	0,00102111	0,00154271	0,00161866	0,000128392	0,000308254	0,000600801	0,0010208	0,00154145	0,0016045
0,7	0,000109415	0,00026715	0,000528036	0,000907492	0,00138102	0,00139555	0,000109349	0,000267103	0,000527926	0,0009072	0,00137973	0,0013815
0,72	9,32E-05	0,000231599	0,000464021	0,000806577	0,001236	0,00119706	9,31E-05	0,000231558	0,000463917	0,00080635	0,00123487	0,00118533
0,74	7,95E-05	0,000200784	0,000407751	0,000716876	0,00110609	0,00102323	7,94E-05	0,000200746	0,000407662	0,000716669	0,00110519	0,00101347
0,76	6,78E-05	0,000174001	0,000358271	0,000637166	0,000989745	0,000871985	6,78E-05	0,000173973	0,000358194	0,000636991	0,000989027	0,00086339
0,78	5,78E-05	0,000150766	0,000314787	0,000566327	0,000885586	0,000741108	5,78E-05	0,000150748	0,000314723	0,000566198	0,000884972	0,000733589
0,8	4,93E-05	0,000130663	0,000276594	0,000503378	0,000792365	0,000628577	4,93E-05	0,000130649	0,000276542	0,000503276	0,000791784	0,00062184
0,82	4,20E-05	0,000113264	0,000243046	0,000447446	0,000708917	0,000531967	4,20E-05	0,00011325	0,000243002	0,000447366	0,000708387	0,00052605
0,84	3,58E-05	9,82E-05	0,000213562	0,00039774	0,000634211	0,000449366	3,58E-05	9,82E-05	0,000213526	0,000397676	0,000633673	0,00044408
0,86	3,06E-05	8,51E-05	0,000187649	0,000353548	0,000567307	0,000379121	3,05E-05	8,51E-05	0,000187621	0,000353498	0,00056681	0,00037427
0,88	2,60E-05	7,37E-05	0,000164882	0,000314252	0,000507429	0,000319453	2,60E-05	7,37E-05	0,00016486	0,000314209	0,000506962	0,000315171
0,9	2,22E-05	6,39E-05	0,000144882	0,000279309	0,000453819	0,00026891	2,22E-05	6,39E-05	0,000144864	0,000279272	0,000453368	0,000265142
0,92	1,89E-05	5,54E-05	0,000127309	0,000248243	0,000405832	0,000226111	1,89E-05	5,54E-05	0,000127295	0,000248211	0,000405419	0,000222865
0,94	1,61E-05	4,80E-05	0,000111867	0,000220627	0,000362913	0,00018999	1,61E-05	4,80E-05	0,000111855	0,0002206	0,000362542	0,000187111
0,96	1,38E-05	4,16E-05	9,83E-05	0,000196082	0,000324523	0,000159456	1,38E-05	4,16E-05	9,83E-05	0,000196056	0,000324205	0,000156998
0,98	1,17E-05	3,60E-05	8,64E-05	0,000174265	0,000290184	0,000133718	1,17E-05	3,60E-05	8,64E-05	0,000174242	0,000289913	0,000131637
1	1,00E-05	3,12E-05	7,59E-05	0,000154876	0,000259466	0,000112059	1,00E-05	3,12E-05	7,59E-05	0,000154854	0,000259234	0,000110304

Hydrodynamic Force

Time [s]	Hydrodynamic Force [μN]											
	Particle 1						Particle 2					
	$\rho = 1000$	$\rho = 1500$	$\rho = 2000$	$\rho = 2500$	$\rho = 3000$	$\rho = 3500$	$\rho = 1000$	$\rho = 1500$	$\rho = 2000$	$\rho = 2500$	$\rho = 3000$	$\rho = 3500$
0	0	0	0	0	0	0	0	0	0	0	0	0
0,02	-138,713	-92,3745	-45,6659	-49,2104	-80,0075	-177,254	280,729	340,62	367,26	387,055	411,581	487,649
0,04	-128,801	-325,506	-194,109	-184,239	-245,227	-295,067	67,5481	217,762	69,5086	58,2756	84,7801	107,689
0,06	-61,4239	-28,5385	-34,1556	-65,105	-70,7819	-59,3425	19,4788	-14,0429	-25,4495	-5,75753	10,4176	18,3941
0,08	-4,13618	-26,1381	-59,5281	-94,1545	-110,011	-117,505	-27,8187	-54,5324	-63,17	-71,9554	-77,0284	-80,1188
0,1	2,13087	4,74228	9,50382	16,4061	22,3307	29,9962	-11,5967	5,95828	28,9424	38,2776	39,9593	36,0819
0,12	5,25318	1,40892	-5,5415	-13,0662	-21,1839	-26,3293	9,05622	10,3571	6,42269	3,4916	1,87767	-1,92436
0,14	1,35332	-4,24398	-11,1474	-20,3909	-32,5546	-41,3941	-0,695853	-5,74842	-16,5584	-29,5931	-39,8321	-50,5452
0,16	-6,20171	-16,3813	-22,5071	-26,4481	-27,9942	-29,1571	-7,54438	-16,5212	-21,6832	-23,9175	-23,4392	-23,1514
0,18	-6,34658	-5,91178	-4,21428	-4,02231	-6,42639	-11,7717	-5,92023	-4,3337	-3,87018	-5,7773	-10,0838	-15,5354
0,2	-0,280597	0,432459	-0,577819	-2,98703	-6,39471	-9,41331	-0,121588	0,747055	-0,622346	-4,24295	-8,29782	-10,8973
0,22	1,39108	0,0454376	-3,83874	-7,61035	-10,9432	-13,6836	1,11492	-0,663574	-4,45741	-8,04155	-10,2718	-13,7183
0,24	-0,801773	-4,7407	-8,18746	-10,9427	-14,3751	-17,6813	-0,759022	-4,49344	-7,29733	-10,0712	-13,2209	-16,3775
0,26	-2,50325	-4,38014	-5,74793	-7,73461	-9,87866	-12,0127	-2,41556	-4,1643	-5,68721	-7,66561	-9,5907	-12,0477
0,28	-1,6155	-1,72816	-2,36147	-3,7802	-6,1506	-9,31516	-1,63578	-1,75524	-2,53981	-4,06347	-6,40026	-9,78496
0,3	-0,231055	-0,349912	-1,72805	-3,68988	-5,92362	-8,07802	-0,2497	-0,47462	-1,89153	-3,92282	-6,29303	-8,52066
0,32	0,0468793	-1,25096	-3,01915	-4,77813	-6,42219	-8,29568	0,0607298	-1,23083	-2,98284	-4,69904	-6,21048	-8,28785
0,34	-0,540863	-1,92931	-3,21666	-4,58026	-6,31599	-8,31765	-0,535834	-1,90135	-3,09484	-4,38149	-6,08006	-7,98804
0,36	-0,827537	-1,48259	-2,2139	-3,49177	-5,06905	-6,96385	-0,828434	-1,44854	-2,18054	-3,47629	-5,04294	-6,96542
0,38	-0,532945	-0,710302	-1,43801	-2,60652	-4,10713	-6,14582	-0,530553	-0,719144	-1,48871	-2,69943	-4,23996	-6,22684
0,4	-0,160924	-0,538885	-1,40665	-2,46108	-3,75821	-5,48742	-0,160862	-0,56226	-1,43816	-2,48755	-3,81472	-5,46885
0,42	-0,119823	-0,755025	-1,55454	-2,48443	-3,57583	-5,13659	-0,121298	-0,754361	-1,52486	-2,45311	-3,53396	-5,07807
0,44	-0,261797	-0,798561	-1,39682	-2,22655	-3,31929	-4,80236	-0,261163	-0,780185	-1,37345	-2,19213	-3,24717	-4,68649
0,46	-0,300831	-0,576807	-1,06376	-1,85594	-2,87855	-4,32182	-0,298606	-0,570791	-1,06619	-1,85454	-2,87086	-4,31197
0,48	-0,19502	-0,380347	-0,858068	-1,56528	-2,52037	-3,86782	-0,194095	-0,386273	-0,869408	-1,57883	-2,52496	-3,91227
0,5	-0,0965655	-0,351176	-0,813559	-1,43038	-2,24628	-3,54262	-0,0970564	-0,355878	-0,817015	-1,44027	-2,27235	-3,55405
0,52	-0,0885035	-0,379043	-0,776841	-1,324	-2,05242	-3,23021	-0,0889902	-0,37669	-0,76978	-1,31666	-2,04598	-3,23357
0,54	-0,118287	-0,341795	-0,672544	-1,17617	-1,85905	-2,9413	-0,118072	-0,338009	-0,667335	-1,16763	-1,8523	-2,95314
0,56	-0,114821	-0,258846	-0,553361	-1,02264	-1,66434	-2,68956	-0,114362	-0,258638	-0,555206	-1,0232	-1,65585	-2,68268
0,58	-0,0789962	-0,203769	-0,477919	-0,895361	-1,47781	-2,44178	-0,0788299	-0,205574	-0,480451	-0,897297	-1,47785	-2,43281
0,6	-0,051404	-0,190362	-0,436518	-0,802732	-1,32093	-2,15819	-0,0515364	-0,190859	-0,437025	-0,803234	-1,32268	-2,19848
0,62	-0,0481372	-0,181233	-0,39391	-0,722379	-1,19065	-1,97832	-0,0482338	-0,180146	-0,392023	-0,720545	-1,1866	-1,96852
0,64	-0,0519991	-0,15498	-0,340899	-0,642572	-1,07184	-1,77532	-0,0519136	-0,154124	-0,339993	-0,641133	-1,06823	-1,76406
0,66	-0,0463794	-0,124476	-0,291906	-0,567074	-0,959038	-1,57233	-0,0462449	-0,124636	-0,292441	-0,566986	-0,957866	-1,56714
0,68	-0,0340519	-0,105584	-0,256708	-0,501796	-0,858073	-1,38902	-0,0340205	-0,10603	-0,257239	-0,502479	-0,85809	-1,3894
0,7	-0,0255804	-0,0961988	-0,229874	-0,447195	-0,768763	-1,23337	-0,0256248	-0,0962166	-0,229651	-0,447122	-0,769201	-1,22722
0,72	-0,0235497	-0,0862978	-0,203422	-0,399374	-0,688913	-1,09187	-0,0235599	-0,0860188	-0,202958	-0,398939	-0,687376	-1,07467
0,74	-0,0227863	-0,0731871	-0,177011	-0,355013	-0,617827	-0,95126	-0,0227478	-0,0730442	-0,176884	-0,354623	-0,616933	-0,941484
0,76	-0,0195432	-0,0612261	-0,154146	-0,314473	-0,55366	-0,825627	-0,0195053	-0,0613049	-0,154283	-0,31431	-0,55266	-0,81823
0,78	-0,0151478	-0,0531894	-0,135862	-0,279011	-0,495226	-0,712042	-0,0151408	-0,0532792	-0,135933	-0,278971	-0,494711	-0,705797
0,8	-0,0122209	-0,0473781	-0,120289	-0,248218	-0,443059	-0,611409	-0,012229	-0,047352	-0,120181	-0,24816	-0,442787	-0,606174
0,82	-0,0110059	-0,0414431	-0,105799	-0,220972	-0,396501	-0,523855	-0,0110042	-0,041372	-0,105689	-0,220737	-0,396391	-0,519359
0,84	-0,0100263	-0,035336	-0,0925131	-0,19638	-0,355267	-0,446474	-0,0100134	-0,0353184	-0,0924927	-0,196272	-0,355127	-0,443529
0,86	-0,00847591	-0,0302098	-0,0810611	-0,174442	-0,318022	-0,379849	-0,00846535	-0,0302365	-0,0810854	-0,174398	-0,317774	-0,375953
0,88	-0,00682566	-0,026363	-0,0713799	-0,155029	-0,284729	-0,3219	-0,00682372	-0,0263772	-0,0713776	-0,155028	-0,284531	-0,318353
0,9	-0,00569548	-0,0231451	-0,0628971	-0,137899	-0,254887	-0,272581	-0,00569661	-0,0231298	-0,062865	-0,137882	-0,254675	-0,269417
0,92	-0,00503584	-0,0200623	-0,0552484	-0,12266	-0,227948	-0,23055	-0,00503399	-0,0200455	-0,0552233	-0,12263	-0,227827	-0,22764
0,94	-0,00443951	-0,017222	-0,0484435	-0,109034	-0,203915	-0,194721	-0,00443528	-0,0172215	-0,0484398	-0,109006	-0,203668	-0,192077
0,96	-0,00374172	-0,0148663	-0,042538	-0,0968758	-0,182411	-0,164191	-0,00373872	-0,0148729	-0,042541	-0,0968653	-0,182158	-0,16194
0,98	-0,00308802	-0,0129556	-0,037422	-0,0860862	-0,163173	-0,138316	-0,00308732	-0,0129563	-0,0374179	-0,0860753	-0,162954	-0,136263
1	-0,0026156	-0,0112866	-0,0329143	-0,0765145	-0,145963	-0,11631	-0,00261547	-0,0112815	-0,0329055	-0,0765142	-0,145787	-0,114541

Variation of Initial Velocity

Change the x-component of the sphereVelocity corresponding to $\mathbf{u}_{p,0}$ to a value of choice.

```
. . .

//Particle Settings
T centerX = 0.0075;
T centerY = lengthY*.5;
T centerZ = lengthZ*.5;
T const sphereDensity = 2500;
T const sphereRadius = 0.002;
Vector<T,3> sphereCenter = {centerX,centerY,centerZ};
Vector<T,3> sphereVelocity = {0.3,0.,0.};
Vector<T,3> externalAcceleration = {0., 0., 0.};

. . .
```

Time [s]	Hydrodynamic Force [μN]					
	Particle 1			Particle 2		
	v = 0.1	v = 0.2	v = 0.3	v = 0.1	v = 0.2	v = 0.3
0	0	0	0	0	0	0
0,02	-36,535	-44,5248	-49,2104	188,681	261,747	387,055
0,04	-67,8997	-273,119	-184,239	18,2406	86,8111	58,2756
0,06	-33,3553	-35,7979	-65,105	11,1828	0,693944	-5,75753
0,08	-21,2481	-32,1921	-94,1545	-9,97157	-45,0799	-71,9554
0,1	-18,9349	4,93612	16,4061	24,8895	21,5614	38,2776
0,12	-27,763	-12,4584	-13,0662	25,7332	-1,82659	3,4916
0,14	-8,3753	-12,0759	-20,3909	-2,93972	-15,8096	-29,5931
0,16	-9,58341	-17,6457	-26,4481	-8,79351	-17,716	-23,9175
0,18	-2,51319	-3,11595	-4,02231	-1,9316	-2,31986	-5,7773
0,2	-0,516444	-2,05264	-2,98703	-1,16713	-2,00668	-4,24295
0,22	-2,84226	-5,91677	-7,61035	-2,60217	-6,35649	-8,04155
0,24	-3,93725	-7,85291	-10,9427	-3,81523	-7,41481	-10,0712
0,26	-2,27949	-4,40754	-7,73461	-2,34246	-4,46584	-7,66561
0,28	-1,23243	-2,25792	-3,7802	-1,20059	-2,48134	-4,06347
0,3	-1,45263	-2,86405	-3,68988	-1,4073	-2,90585	-3,92282
0,32	-1,83892	-3,70611	-4,77813	-1,84465	-3,62367	-4,69904
0,34	-1,53687	-3,05214	-4,58026	-1,53708	-3,00072	-4,38149
0,36	-1,03252	-2,01363	-3,49177	-1,02533	-2,04604	-3,47629
0,38	-0,90629	-1,75998	-2,60652	-0,900465	-1,77662	-2,69943
0,4	-0,98551	-1,92529	-2,46108	-0,981855	-1,91964	-2,48755
0,42	-0,917596	-1,81425	-2,48443	-0,915715	-1,78434	-2,45311
0,44	-0,71979	-1,43422	-2,22655	-0,718121	-1,43505	-2,19213
0,46	-0,598005	-1,17611	-1,85594	-0,597434	-1,19047	-1,85454
0,48	-0,575394	-1,11437	-1,56528	-0,574878	-1,11335	-1,57883
0,5	-0,542301	-1,06052	-1,43038	-0,541264	-1,05409	-1,44027
0,52	-0,463412	-0,922057	-1,324	-0,462233	-0,919824	-1,31666
0,54	-0,390977	-0,775164	-1,17617	-0,38984	-0,778697	-1,16763
0,56	-0,353673	-0,68948	-1,02264	-0,353042	-0,690472	-1,0232
0,58	-0,326679	-0,635103	-0,895361	-0,326407	-0,633429	-0,897297
0,6	-0,288944	-0,570821	-0,802732	-0,288818	-0,569055	-0,803234
0,62	-0,249304	-0,495502	-0,722379	-0,249146	-0,495802	-0,720545
0,64	-0,220594	-0,434527	-0,642572	-0,220468	-0,435182	-0,641133
0,66	-0,199734	-0,390381	-0,567074	-0,199666	-0,390756	-0,566986
0,68	-0,178572	-0,351529	-0,501796	-0,17851	-0,351003	-0,502479
0,7	-0,156757	-0,311363	-0,447195	-0,156697	-0,311177	-0,447122
0,72	-0,138267	-0,274038	-0,399374	-0,138252	-0,274042	-0,398939
0,74	-0,123739	-0,243463	-0,355013	-0,123677	-0,243483	-0,354623
0,76	-0,110645	-0,217812	-0,314473	-0,110589	-0,217636	-0,31431
0,78	-0,0979388	-0,193925	-0,279011	-0,097883	-0,193738	-0,278971
0,8	-0,0865246	-0,171603	-0,248218	-0,0864724	-0,17154	-0,24816
0,82	-0,0769471	-0,152069	-0,220972	-0,0769072	-0,152079	-0,220737
0,84	-0,0686224	-0,135408	-0,19638	-0,0685872	-0,135394	-0,196272
0,86	-0,0609521	-0,120642	-0,174442	-0,0609222	-0,120599	-0,174398
0,88	-0,0539893	-0,107167	-0,155029	-0,0539659	-0,107139	-0,155028
0,9	-0,0479318	-0,095081	-0,137899	-0,0479125	-0,0950813	-0,137882
0,92	-0,0426579	-0,0845073	-0,12266	-0,0426427	-0,0845119	-0,12263
0,94	-0,0379239	-0,075212	-0,109034	-0,0379117	-0,075205	-0,109006
0,96	-0,0336496	-0,0668832	-0,0968758	-0,0336399	-0,0668724	-0,0968653
0,98	-0,0298668	-0,0594026	-0,0860862	-0,029859	-0,0593984	-0,0860753
1	-0,0265472	-0,0527663	-0,0765145	-0,026541	-0,0527667	-0,0765142

Collision with both spheres in motion

Change the vectors for creation of particle indicators and particle velocity after initialization of particleIndicator1:

```
. . .

    int main(int argc, char* argv[])
{
. . .

    //Sphere indicator
    SmoothIndicatorSphere3D<T, T, true> particleIndicator1(...);
    sphereCenter[0] = 0.0225;
    sphereCenter[1] = lengthY*.5;
    sphereCenter[2] = lengthZ*.5;
    sphereVelocity[0] = -0.3;
    SmoothIndicatorSphere3D<T, T, true> particleIndicator2(...);

. . .
}
```

Time [s]	Velocity in x-Direction [m/s]		Hydrodynamic Force [μN]	
	Particle 1	Particle 2	Particle 1	Particle 2
0	0,3	-0,3	0	0
0,02	0,142346	-0,142346	-421,52	421,52
0,04	0,0190245	-0,0190245	-2252,1	2252,1
0,06	0,00081625	-0,00081625	13,261	-13,261
0,08	4,58E-05	-4,58E-05	55,515	-55,515
0,1	1,88E-05	-1,88E-05	-4,68187	4,68187
0,12	9,95E-05	-9,95E-05	-0,821911	0,821911
0,14	2,45E-05	-2,45E-05	5,87642	-5,87642
0,16	1,26E-06	-1,26E-06	-2,6167	2,6167
0,18	1,97E-05	-1,97E-05	-2,15648	2,15648
0,2	1,35E-05	-1,35E-05	1,11144	-1,11144
0,22	3,08E-06	-3,08E-06	0,325382	-0,325382
0,24	4,03E-06	-4,03E-06	-0,382917	0,382917
0,26	4,28E-06	-4,28E-06	0,00207352	-0,00207352
0,28	2,09E-06	-2,09E-06	0,118029	-0,118029
0,3	1,40E-06	-1,40E-06	-0,0463173	0,0463173
0,32	1,39E-06	-1,39E-06	-0,0286683	0,0286683
0,34	9,73E-07	-9,73E-07	0,0192895	-0,0192895
0,36	6,30E-07	-6,30E-07	0,00132864	-0,00132864
0,38	5,24E-07	-5,24E-07	-0,00803859	0,00803859
0,4	4,14E-07	-4,14E-07	0,000605122	-0,000605122
0,42	2,95E-07	-2,95E-07	0,00146838	-0,00146838
0,44	2,26E-07	-2,26E-07	-0,00134823	0,00134823
0,46	1,80E-07	-1,80E-07	-0,00058842	0,000588419
0,48	1,37E-07	-1,37E-07	0,000191212	-0,000191211
0,5	1,05E-07	-1,05E-07	-0,000172363	0,000172362
0,52	8,28E-08	-8,28E-08	-0,000244402	0,000244402
0,54	6,47E-08	-6,47E-08	-5,42496E-05	5,42507E-05
0,56	5,03E-08	-5,03E-08	-4,58539E-05	4,58533E-05
0,58	3,96E-08	-3,96E-08	-7,75065E-05	0,000077507
0,6	3,13E-08	-3,13E-08	-4,68862E-05	4,68864E-05
0,62	2,47E-08	-2,47E-08	-2,76509E-05	2,76508E-05
0,64	1,95E-08	-1,95E-08	-2,86988E-05	0,000028699
0,66	1,55E-08	-1,55E-08	-2,35523E-05	0,000023552
0,68	1,23E-08	-1,23E-08	-1,61828E-05	1,61829E-05
0,7	9,82E-09	-9,82E-09	-1,33055E-05	1,33058E-05
0,72	7,84E-09	-7,84E-09	-1,12568E-05	1,12568E-05
0,74	6,27E-09	-6,27E-09	-8,6661E-06	8,66593E-06
0,76	5,03E-09	-5,03E-09	-6,83896E-06	6,83905E-06
0,78	4,03E-09	-4,03E-09	-5,63473E-06	5,63482E-06
0,8	3,24E-09	-3,24E-09	-4,53793E-06	4,53788E-06
0,82	2,61E-09	-2,61E-09	-3,62715E-06	3,62716E-06
0,84	2,10E-09	-2,10E-09	-2,95494E-06	2,95476E-06
0,86	1,69E-09	-1,69E-09	-2,4115E-06	2,4115E-06
0,88	1,37E-09	-1,37E-09	-1,95922E-06	1,95916E-06
0,9	1,11E-09	-1,11E-09	-1,60103E-06	1,60107E-06
0,92	8,95E-10	-8,95E-10	-1,31496E-06	1,31501E-06
0,94	7,25E-10	-7,25E-10	-1,08103E-06	1,08092E-06
0,96	5,88E-10	-5,88E-10	-8,90878E-07	8,90934E-07
0,98	4,77E-10	-4,77E-10	-7,37621E-07	7,37809E-07
1	3,88E-10	-3,88E-10	-6,12401E-07	6,12269E-07

Oblique Impact

Change centerY = lengthY*0.5 to centerY = lengthY*0.375;
Change centerY back to centerY = lengthY*0.5 in main function after the first sphere indicator is set:

```
. . .

//Particle Settings
T centerX = 0.0075;
T centerY = lengthY*.375;
T centerZ = lengthZ*.5;
. . .

int main(int argc, char* argv[])
{
. . .

//Sphere indicator
  SmoothIndicatorSphere3D<T, T, true> particleIndicator1(..);
  sphereCenter[0] = 0.015;
  sphereCenter[1] = lengthY*.5;
  sphereCenter[2] = lengthZ*.5;
  sphereVelocity[0] = 0;
  SmoothIndicatorSphere3D<T, T, true> particleIndicator2(..);
. . .
}
```

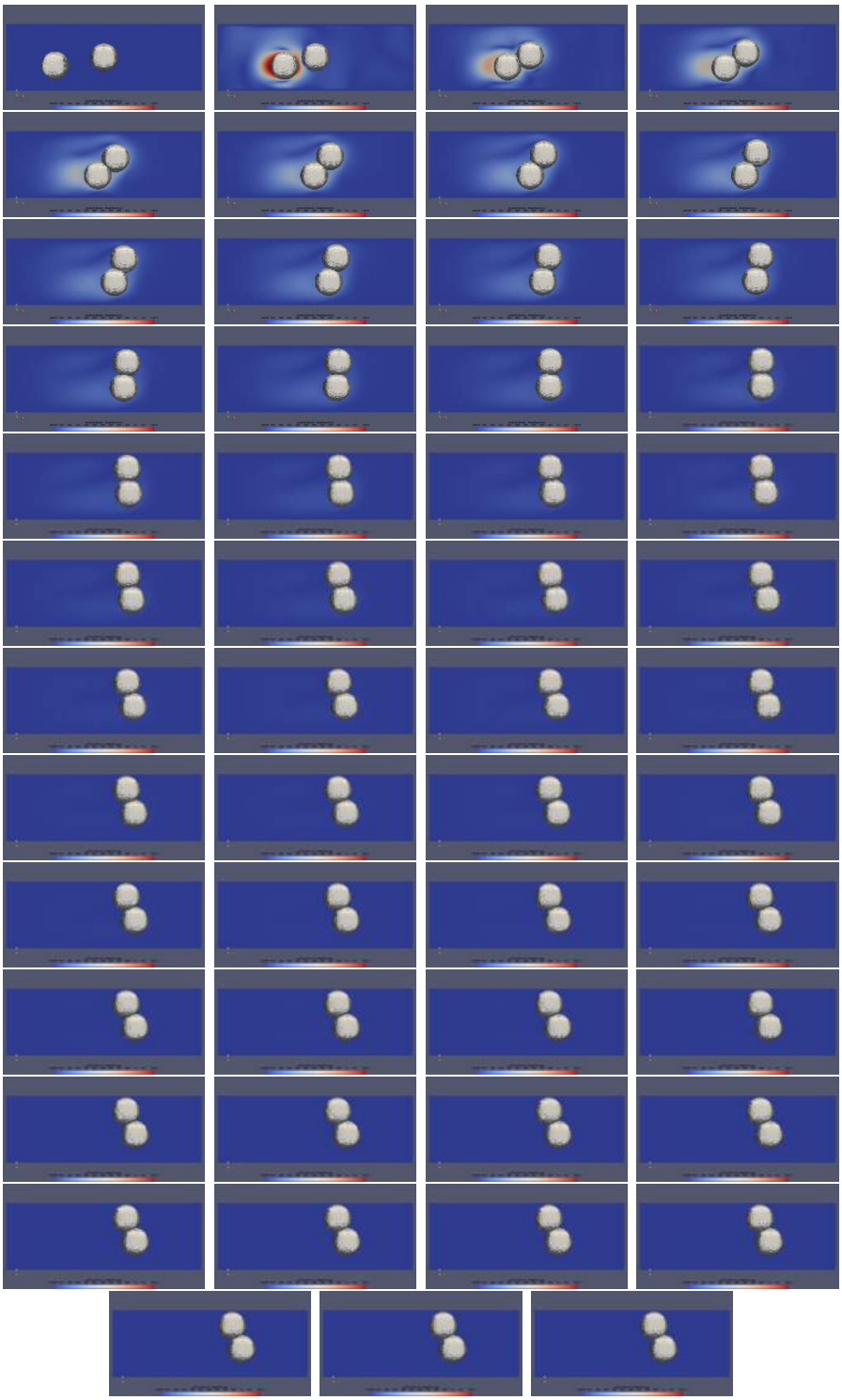

Figure 12: Oblique Impact: Animation of the oblique collision of two spheres made in ParaView. The rectangular slice of the three-dimensional domain shows the magnitude of physical velocity from blue ($0\frac{m}{s}$) to red ($0.12\frac{m}{s}$).

Time [s]	Velocity in x-Direction [m/s]		Angular Velocity in z-Direction [1/s]		Hydrodynamic Force [μN]	
	Particle 1	Particle 2	Particle 1	Particle 2	Particle 1	Particle 2
0	0,3	0	0	0	0	0
0,02	0,118781	0,00372851	0,054155	0,0268666	79,1248	310,481
0,04	0,0562327	0,0399774	1,7083	3,0759	-206,641	49,7058
0,06	0,0493396	0,0324593	2,98046	5,1216	-40,197	-12,8377
0,08	0,0431253	0,0260442	3,35238	5,38597	-84,4448	-60,9363
0,1	0,0366259	0,019775	3,26425	5,12922	17,805	38,7256
0,12	0,0311745	0,0146701	3,07248	4,75822	-5,03191	10,2256
0,14	0,0269044	0,0111717	2,90072	4,36853	-42,2601	-34,4931
0,16	0,0235565	0,00873529	2,73339	3,8895	-22,6253	-20,3041
0,18	0,0201684	0,00647146	2,55414	3,53604	-4,88057	1,41025
0,2	0,0172002	0,0045897	2,31376	3,14341	-3,60918	0,203195
0,22	0,0148044	0,00333638	2,14658	2,75901	-14,0867	-9,09733
0,24	0,0128145	0,0024838	2,01197	2,44321	-11,5371	-7,30731
0,26	0,0110398	0,00174332	1,84674	2,19082	-5,22967	-1,33845
0,28	0,00954656	0,00105183	1,57485	1,88611	-3,10249	-0,351258
0,3	0,00822915	0,00061248	1,50536	1,64606	-5,6372	-1,82342
0,32	0,00709365	0,000356364	1,45936	1,51785	-5,79446	-2,41967
0,34	0,00616691	0,000107393	1,31127	1,35754	-3,53625	-0,959971
0,36	0,00534148	-9,30E-05	1,19094	1,21422	-2,46644	0,112295
0,38	0,00462998	-0,000233691	1,09147	1,08326	-2,68278	-0,384788
0,4	0,00402141	-0,000318	1,00095	0,973064	-2,7188	-0,719306
0,42	0,00350809	-0,000386266	0,898335	0,861491	-2,10663	-0,374459
0,44	0,00306283	-0,00044327	0,797847	0,752568	-1,53825	-0,0206882
0,46	0,00267083	-0,000476852	0,715793	0,660398	-1,51621	0,0836061
0,48	0,00231997	-0,000479302	0,661101	0,594725	-1,45307	-0,0674055
0,5	0,00201443	-0,000470401	0,60914	0,540345	-1,25816	-0,0209559
0,52	0,00175104	-0,000460779	0,553798	0,488266	-0,982597	0,0725674
0,54	0,00152153	-0,000446845	0,503285	0,44275	-0,857371	0,112888
0,56	0,00132348	-0,000429156	0,457007	0,400972	-0,776806	0,0667255
0,58	0,00115353	-0,000409803	0,413711	0,361465	-0,684504	0,0586599
0,6	0,00100619	-0,000389512	0,374039	0,32525	-0,573911	0,0876432
0,62	0,000878152	-0,000368822	0,338019	0,292342	-0,486649	0,10133
0,64	0,000767325	-0,000347876	0,305187	0,262287	-0,424957	0,0853764
0,66	0,000672366	-0,000327704	0,274384	0,233716	-0,371411	0,0726705
0,68	0,000590166	-0,000307987	0,246421	0,207731	-0,326154	0,0824625
0,7	0,00051788	-0,000288127	0,222097	0,185304	-0,279405	0,0851015
0,72	0,000454564	-0,000268564	0,200645	0,165809	-0,246576	0,083245
0,74	0,000399404	-0,000249691	0,181239	0,14844	-0,217677	0,0768441
0,76	0,000351398	-0,00023174	0,163483	0,13286	-0,188373	0,0716576
0,78	0,000309312	-0,000214558	0,147623	0,119208	-0,164967	0,0711207
0,8	0,000272696	-0,000198522	0,133032	0,106643	-0,141337	0,0648194
0,82	0,000240811	-0,000183521	0,119747	0,0952497	-0,125959	0,0617654
0,84	0,000212562	-0,000169099	0,108145	0,0855746	-0,111406	0,0582835
0,86	0,000187716	-0,000155549	0,0977199	0,0770144	-0,0974309	0,0547793
0,88	0,000166062	-0,000143073	0,0880986	0,0690689	-0,085017	0,050961
0,9	0,000146922	-0,000131342	0,0795764	0,0621445	-0,0752153	0,0475544
0,92	0,000130043	-0,0001204	0,0719328	0,0560035	-0,0664195	0,0440454
0,94	0,000115174	-0,000110251	0,0650366	0,0505055	-0,0584652	0,0408339
0,96	0,000102073	-0,000100869	0,0587999	0,0455634	-0,051436	0,0378018
0,98	9,05E-05	-9,22E-05	0,0531553	0,0411123	-0,0453532	0,0348389
1	8,03E-05	-8,42E-05	0,0480461	0,0370984	-0,0400559	0,0320198

References

[1] P. L. Bhatnagar, E. P. Gross, and M. Krook. "A Model for Collision Processes in Gases. I. Small Amplitude Processes in Charged and Neutral One-Component Systems". In: *Physical Review* 94.3 (May 1954), pp. 511–525. DOI: 10.1103/PhysRev.94.511.

[2] Martin Hecht and Jens Harting. "Implementation of on-site velocity boundary conditions for D3Q19 lattice Boltzmann". In: (2008), pp. 1–14. DOI: 10.1088/1742-5468/2010/01/P01018. arXiv: 0811.4593.

[3] Mathias J. Krause et al. "Particle flow simulations with homogenised lattice Boltzmann methods". In: *Particuology* 34 (2017), pp. 1–13. DOI: 10.1016/j.partic.2016.11.001.

[4] Timm Krüger et al. *The Lattice Boltzmann Method*. Graduate Texts in Physics. Cham: Springer International Publishing, 2017. ISBN: 978-3-319-44647-9. DOI: 10.1007/978-3-319-44649-3.

[5] Anthony J. C. Ladd. "Numerical simulations of particulate suspensions via a discretized Boltzmann equation. Part 1. Theoretical foundation". In: *Journal of Fluid Mechanics* 271 (July 1994), pp. 285–309. DOI: 10.1017/S0022112094001771.

[6] Anthony J. C. Ladd. "Numerical simulations of particulate suspensions via a discretized Boltzmann equation. Part 2. Numerical results". In: *Journal of Fluid Mechanics* 271 (July 1994), pp. 311–339. DOI: 10.1017/S0022112094001783.

[7] Charles S. Peskin. "The immersed boundary method". In: *Acta Numerica* 11 (Jan. 2002), pp. 479–517. DOI: 10.1017/S0962492902000077.

[8] Michael A.A. Spaid and Frederick R. Phelan. "Lattice Boltzmann methods for modeling microscale flow in fibrous porous media". In: *Physics of Fluids* 9.9 (1997), pp. 2468–2474. DOI: 10.1063/1.869392.

[9] Robin Trunk et al. "Towards the simulation of arbitrarily shaped 3D particles using a homogenised lattice Boltzmann method". In: *Computers and Fluids* 172 (2018), pp. 621–631. DOI: 10.1016/j.compfluid.2018.02.027.